Appendix D: Species Distribution Model Outputs

Essential Fish Habitat Framework

Atlantic Herring Fishery Management Plan

Framework Adjustment 12

Monkfish Fishery Management Plan

Framework Adjustment 18

Northeast Multispecies Fishery Management Plan

Framework Adjustment 70

Northeast Skate Complex Fishery Management Plan

Framework Adjustment 13

Draft

April 9, 2026

Prepared by the

New England Fishery Management Council

In consultation with the

National Marine Fisheries Service

1.0 TABLE OF CONTENTS

1.1 TABLES

1.2 Figures

1.3 Acronyms

CFR	Code of Federal Regulations
EcoMon	Ecosystem Monitoring
EEZ	Exclusive Economic Zone
EFH	Essential Fish Habitat
FMP	Fishery management plan
FW	Framework
GARFO	Greater Atlantic Regional Fisheries Office
GB	Georges Bank
GLOBEC	Global Ocean Ecosystem Dynamics
GOM	Gulf of Maine
HAPC	Habitat Area of Particular Concern
HMA	Habitat Management Area
MADMF	Massachusetts Division of Marine Fisheries
MARMAP	Marine Resources Monitoring and Assessment and Prediction
MSA	Magnuson-Stevens Act; Magnuson-Stevens Fishery Conservation and Management Act
NEFMC	New England Fishery Management Council
NEFSC	Northeast Fisheries Science Center
NEPA	National Environmental Policy Act
NMFS	National Marine Fisheries Service
NOAA	National Oceanic and Atmospheric Administration
SNE	Southern New England
USC	United States Code
WOTUS	Waters of the United States

2.0 INTRODUCTION

The species distribution models that support essential fish habitat (EFH) designation are joint models. Some of the information provided in this document combines results across multiple species and life history stages, and other sections are presented by species. Generally, this information can be used to support EFH consultations as well as other management applications requiring an understanding of species distributions and the environmental drivers of those distributions. Model performance metrics are available upon request.

Note that the model uses a 'hurdle' approach. This means that the model is broken into a presence-absence component and a count component. The presence-absence component uses all observations of survey catch, coding anything greater than zero as present, and zero catches as absent. The count portion of the model uses just the positive catches, retaining the number of fish captured. In Section 1.4: Relationships with Environmental Variables, the results pertaining to these components are presented separately, as they provide slightly different information.

3.0 RELATIONSHIPS WITH ENVIRONMENTAL VARIABLES

The importance of environmental covariates to model predictions was evaluated in two ways, predictor significance (demersal, Figure 1; pelagic, Figure 2) and variance partitioning (demersal, Figure 3; pelagic, Figure 4). The predictor significance plots depict whether covariates are statistically significant at the $p < 0.05$ level using analysis of variance (ANOVA) tests. The variance partitioning plots show how much variance in the response variable (presence/absence or abundance [counts]) is explained by including a given predictor in the model. Each figure has two panels; one illustrates the presence/absence component of the model, and the other illustrates the count component. Taken together, these figures illustrate which environmental covariates are generally important for predicting managed species' habitat.

Then, for each species and life stage, we include smooth-terms figures (Figures 5-20), which illustrate specific relationships between species' presence-absence or density (counts) and individual environmental covariates. Two plots are provided for each species and life stage combination modeled; the first is for the presence/absence component of the model, and the second is for the count component.

Table 1. Environmental covariates used in joint species distribution models (SDMs). Dynamic variables generally use monthly composites.

Model	Variable name	Covariate, data type, resolution	Source and link
Pelagic	SURFTEMP_DOPGLO_monthly_mean	Surface temperature; dynamic	2000-2006: Global Ocean Physics Reanalysis, available via the Copernicus Marine Environmental Monitoring Service (https://doi.org/10.48670/moi-00021) 2007-2019: "DoppioV3R3" ROMs-based (Regional Ocean Modeling System) assimilative reanalysis (Wilkin et al. 2022; https://doi.org/10.1016/j.pocean.2022.102919)
Demersal	BOTTEMP_DOPGLO_monthly_mean	Bottom temperature and salinity; dynamic	
Pelagic	SURFSALIN_DOPGLO_monthly_mean	Surface salinity; dynamic	
Demersal	BOTSALIN_DOPGLO_monthly_mean	Bottom salinity; dynamic	

Model	Variable name	Covariate, data type, resolution	Source and link
Demersal	logGRAIN_km	Log sediment grain size; static	USGS sediment texture & USSEABED databases. https://woodshole.er.usgs.gov/project-pages/sediment/ and https://www.usgs.gov/programs/cmhrp/science/usseabed
Demersal	logDEPTH_km	Log depth; static	NCEI 1-arcsecond Coastal Relief Model. Source: National Centers for Environmental Information https://www.ncei.noaa.gov/products/coastal-relief-model
Demersal	logCOMPLEX_km	Log complexity; static	
Demersal	logBPI_km	Log bathymetric position index; static	
Pelagic	logSURFVELcm_DOP_month_clim_MAG_MEAN	Log surface current velocity; dynamic	2007-2019: "DoppioV3R3" ROMs-based (Regional Ocean Modeling System) assimilative reanalysis (Wilkin et al. 2022; https://doi.org/10.1016/j.pocean.2022.102919)
Demersal	logBOTVELcm_DOP_month_clim_MAG_MEAN	Log wave bottom orbital velocity; dynamic	NREL WPTO wave hindcast, National Renewable Energy Laboratory Water Power Technologies Office https://www.nrel.gov/water/wave-hindcast-dataset
Pelagic, demersal	logTideVel_mean	Log tidal current velocity; dynamic	ADCIRC EC2015 Tidal Database. Includes the M2, S2, N2, K2, O1, K1, Q1, M4, M6 and STEADY tidal constituents. https://adcirc.org/
Pelagic	logMLD_DOPGLO_monthly_MEAN	Log mixed layer depth; dynamic	2000-2006: Global Ocean Physics Reanalysis, available via the Copernicus Marine Environmental Monitoring Service (https://doi.org/10.48670/moi-00021) 2007-2019: "DoppioV3R3" ROMs-based (Regional Ocean Modeling System) assimilative reanalysis (Wilkin et al. 2022; https://doi.org/10.1016/j.pocean.2022.102919)

3.1 Predictor Significance and Variance Partitioning

Figure 1. Predictor significance for demersal species. Statistical significance was evaluated at the p < 0.05 level using analysis of variance (ANOVA) tests for (A) the presence-absence component and (B) the zero-truncated negative binomial component of the joint hurdle species distribution model.

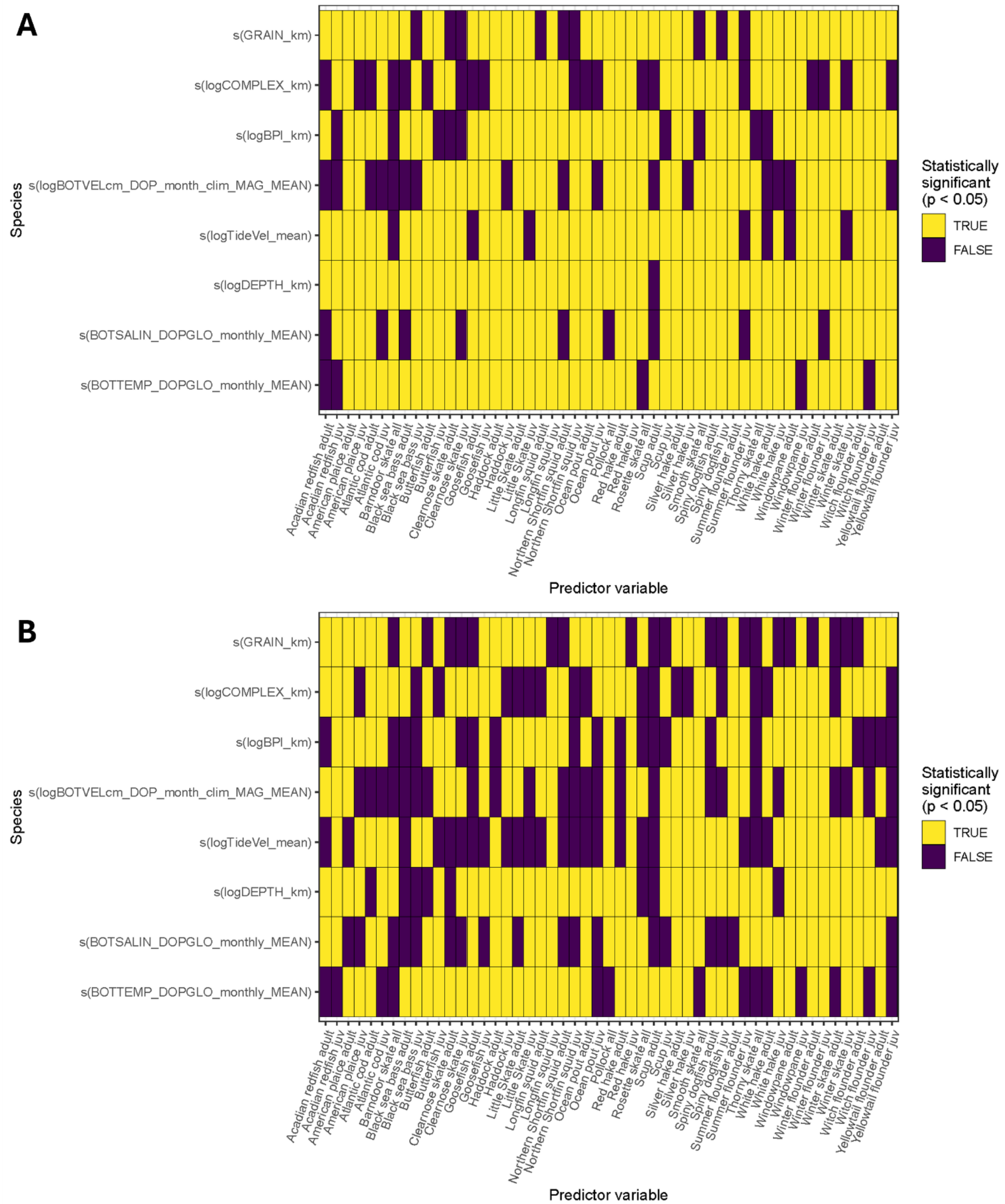

Figure 2. Predictor significance for pelagic species. Statistical significance was evaluated at the $p < 0.05$ level using analysis of variance (ANOVA) tests for (A) the presence-absence component and (B) the zero-truncated negative binomial component of the joint hurdle species distribution model.

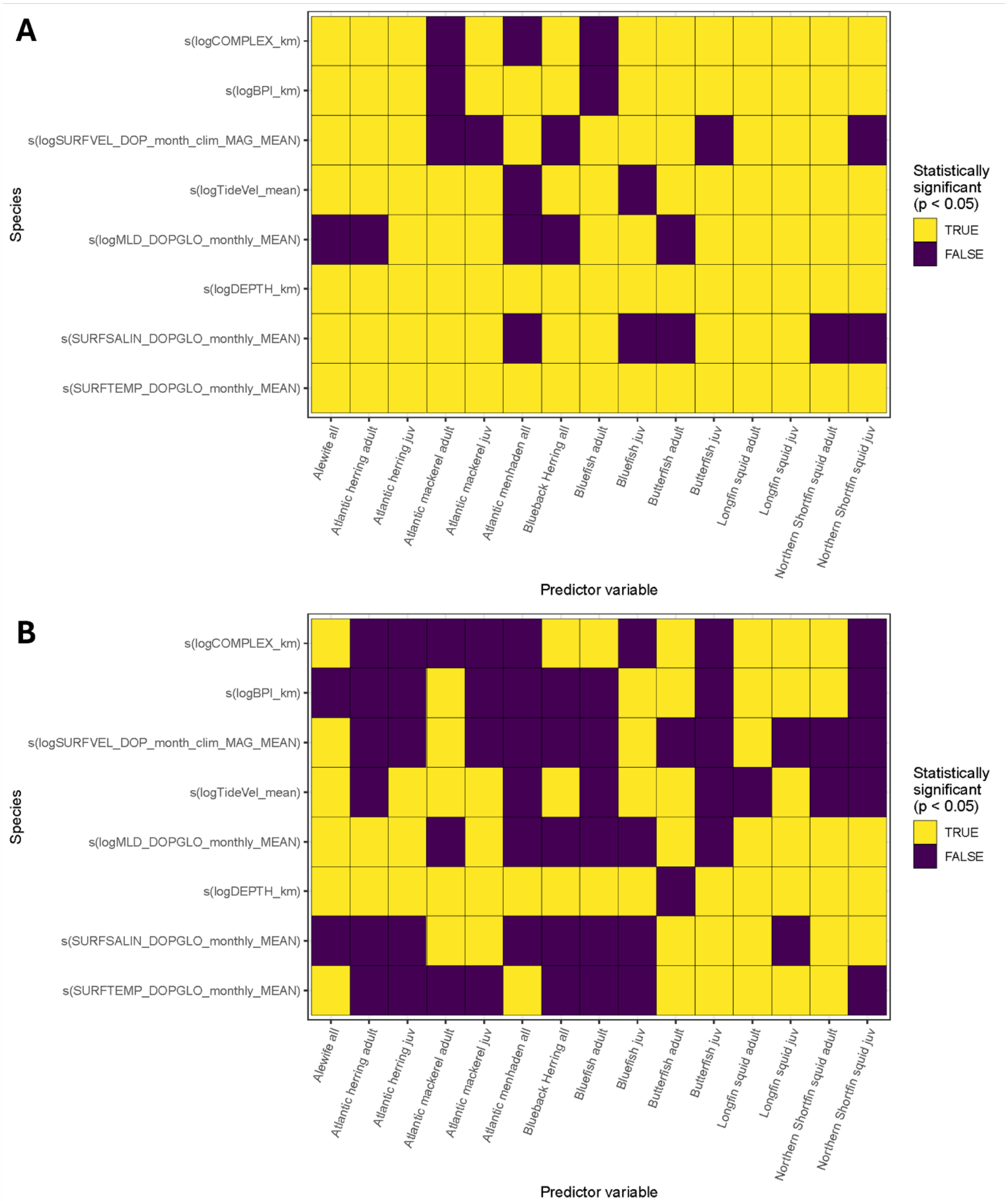

Figure 3. Variance partitioning for demersal species distribution models using a joint hurdle approach. (A) Presence-absence component of the hurdle model. (B) Count (zero-truncated negative binomial component) of the hurdle model.

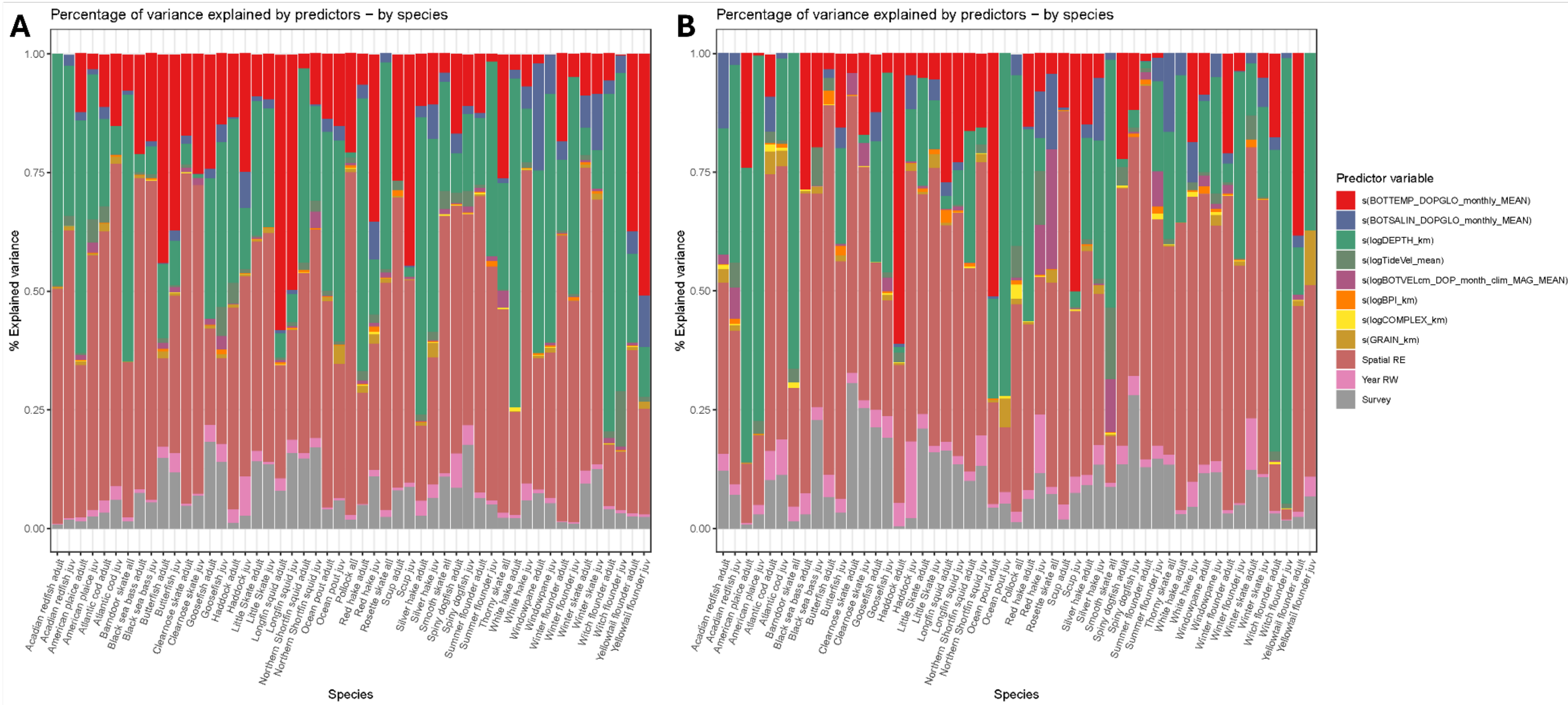

Figure 4. Variance partitioning for pelagic species distribution models using a joint hurdle approach. (A) Presence-absence component of the hurdle model. (B) Zero-truncated negative binomial component of the hurdle model.

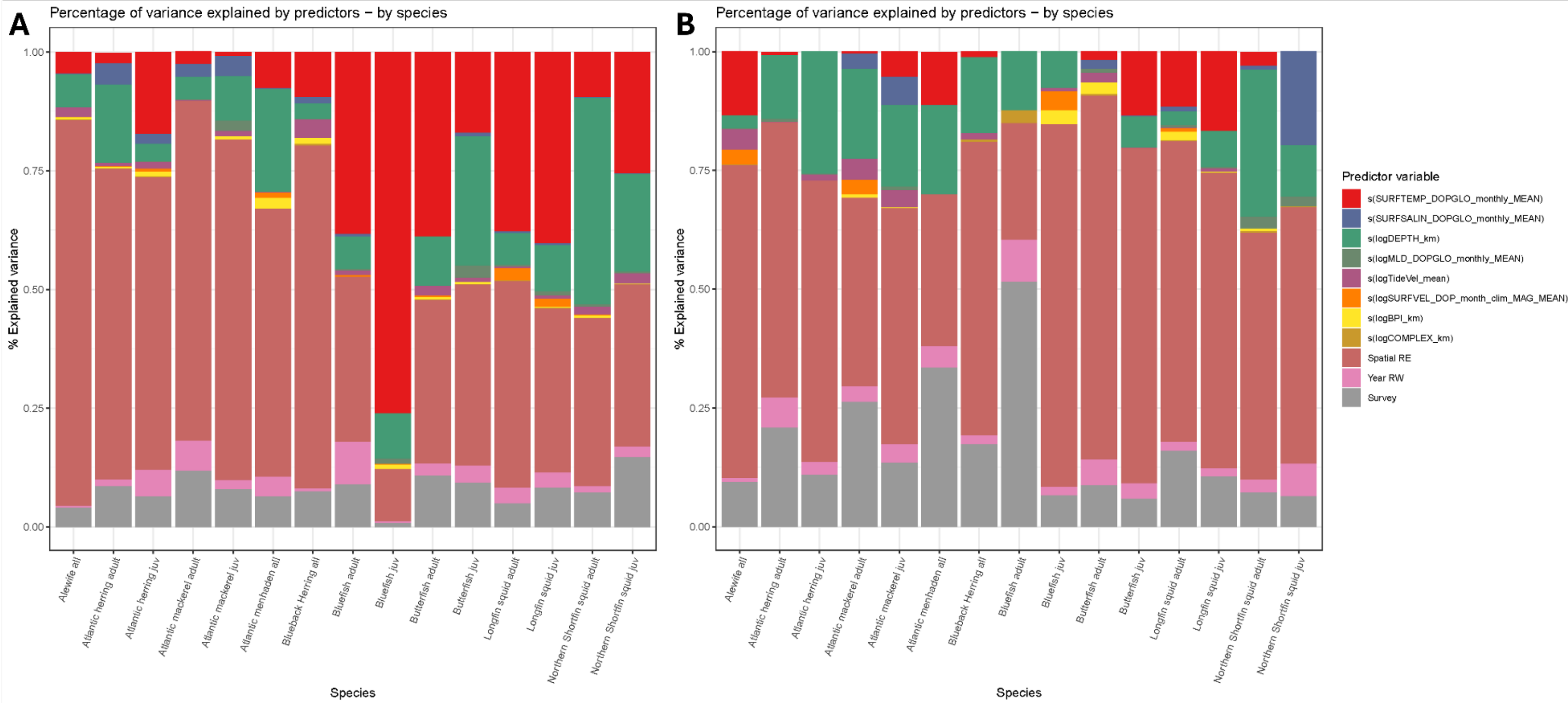

3.2 Smooth Terms: Species-specific relationships

3.2.1 Atlantic cod

Figure 5. Smooth terms graphs depicting relationships between species counts and individual environmental covariates for juvenile Atlantic cod (*Gadus morhua*). (A) Presence-absence component. (B) Zero-truncated negative binomial (count) component of the joint hurdle species distribution model.

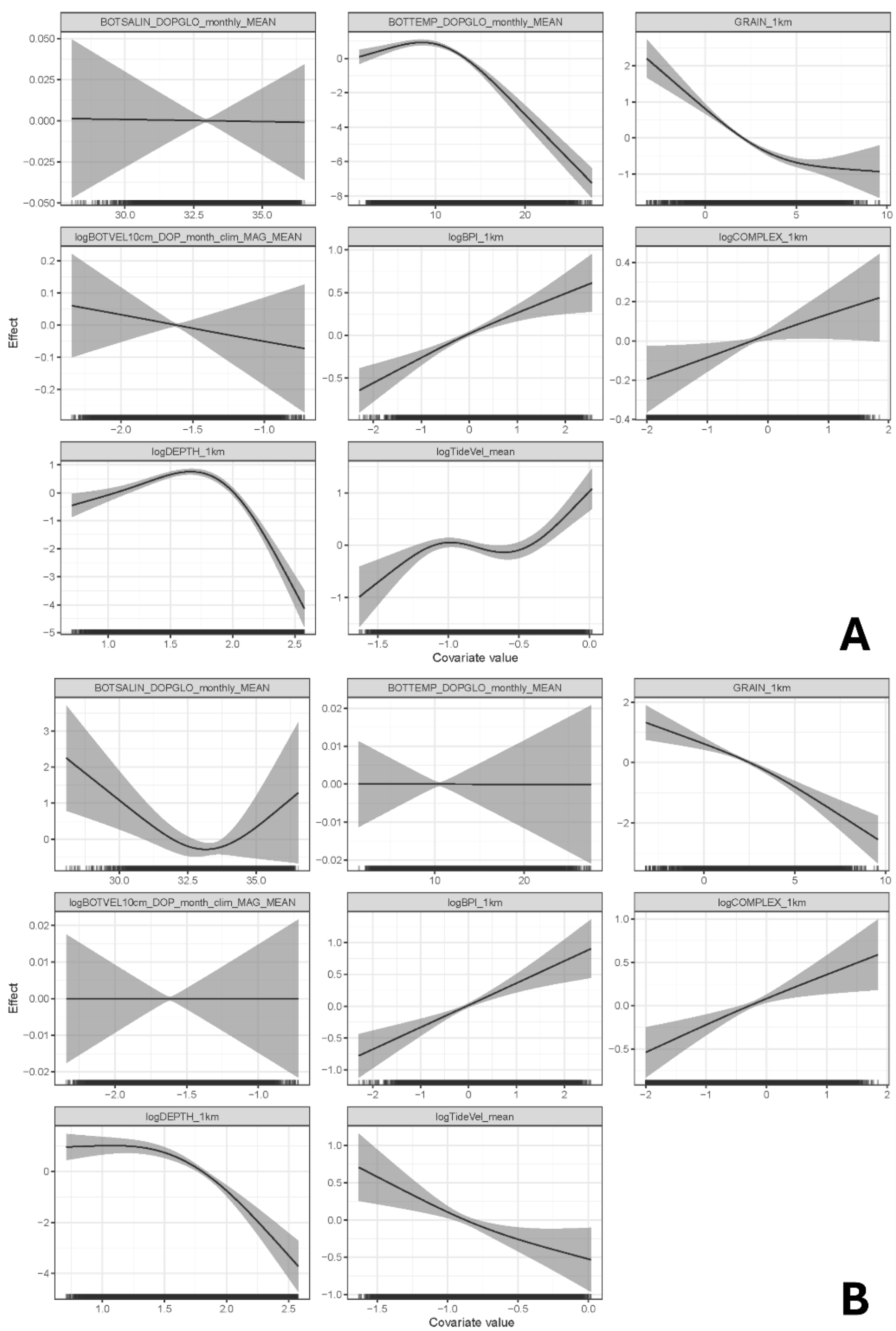

Figure 6. Smooth terms graphs depicting relationships between species counts and individual environmental covariates for adult Atlantic cod (*Gadus morhua*). (A) Presence-absence component. (B) Zero-truncated negative binomial component of the joint hurdle species distribution model.

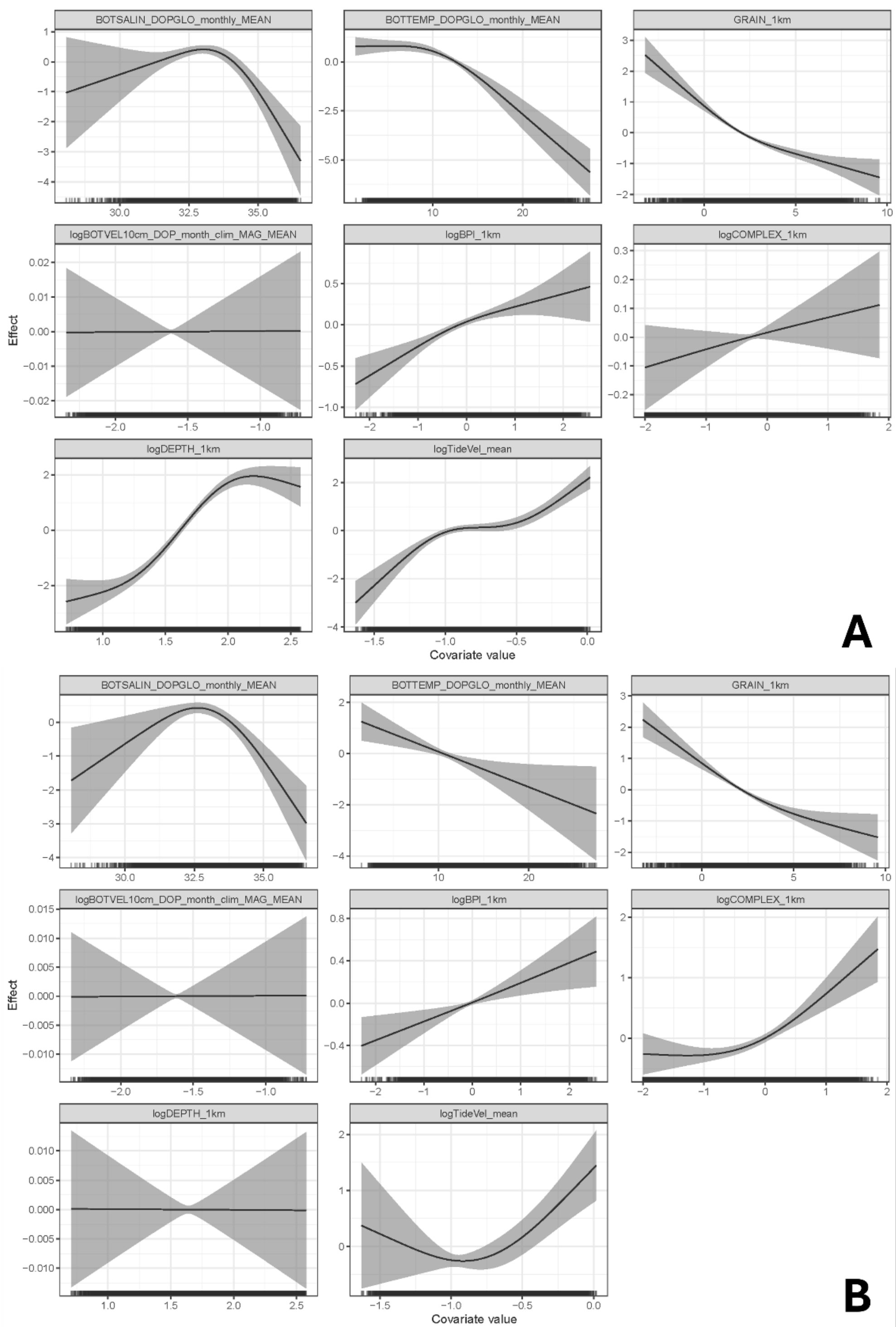

3.2.2 Atlantic herring

Figure 7. Smooth terms graphs depicting relationships between species counts and individual environmental covariates for juvenile Atlantic herring (*Clupea harengus*). (A) Presence-absence component. (B) Zero-truncated negative binomial component of the joint hurdle species distribution model.

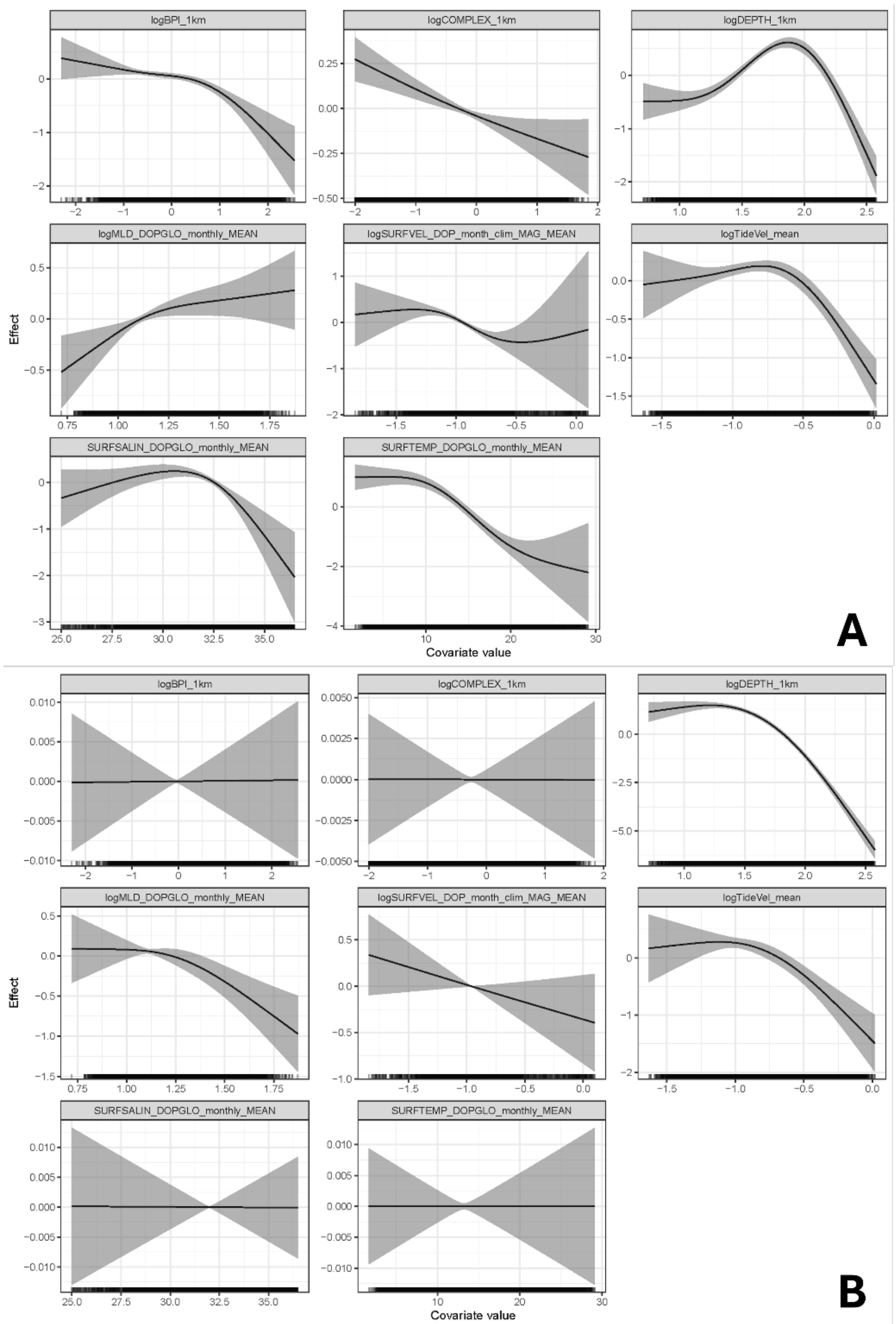

Figure 8. Smooth terms graphs depicting relationships between species counts and individual environmental covariates for adult Atlantic herring (*Clupea harengus*). (A) Presence-absence component. (B) Zero-truncated negative binomial component of the joint hurdle species distribution model.

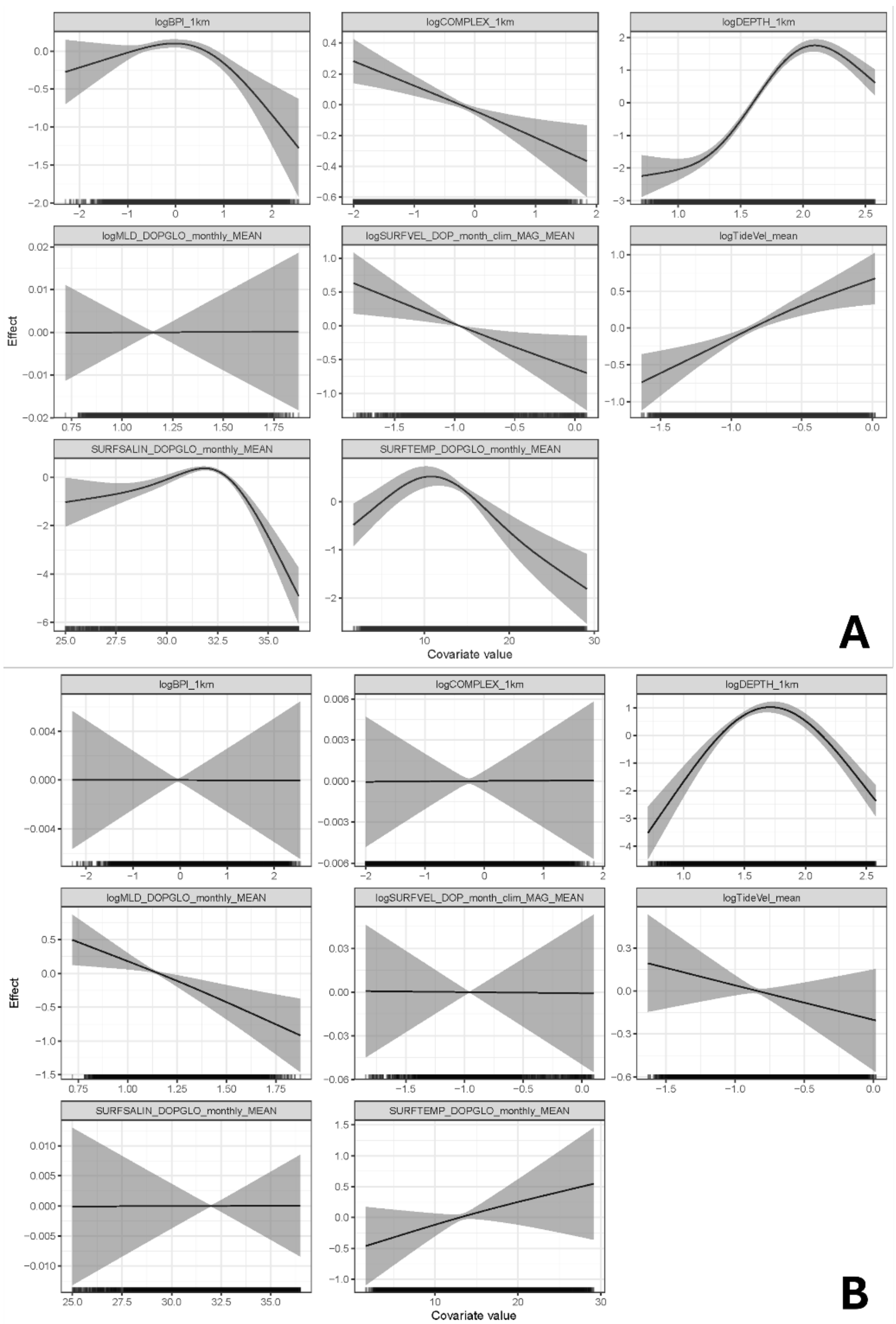

3.2.3 Monkfish

Figure 9. Smooth terms graphs depicting relationships between species counts and individual environmental covariates for juvenile monkfish (*Lophius americanus*). (A) Presence-absence component. (B) Zero-truncated negative binomial component of the joint hurdle species distribution model.

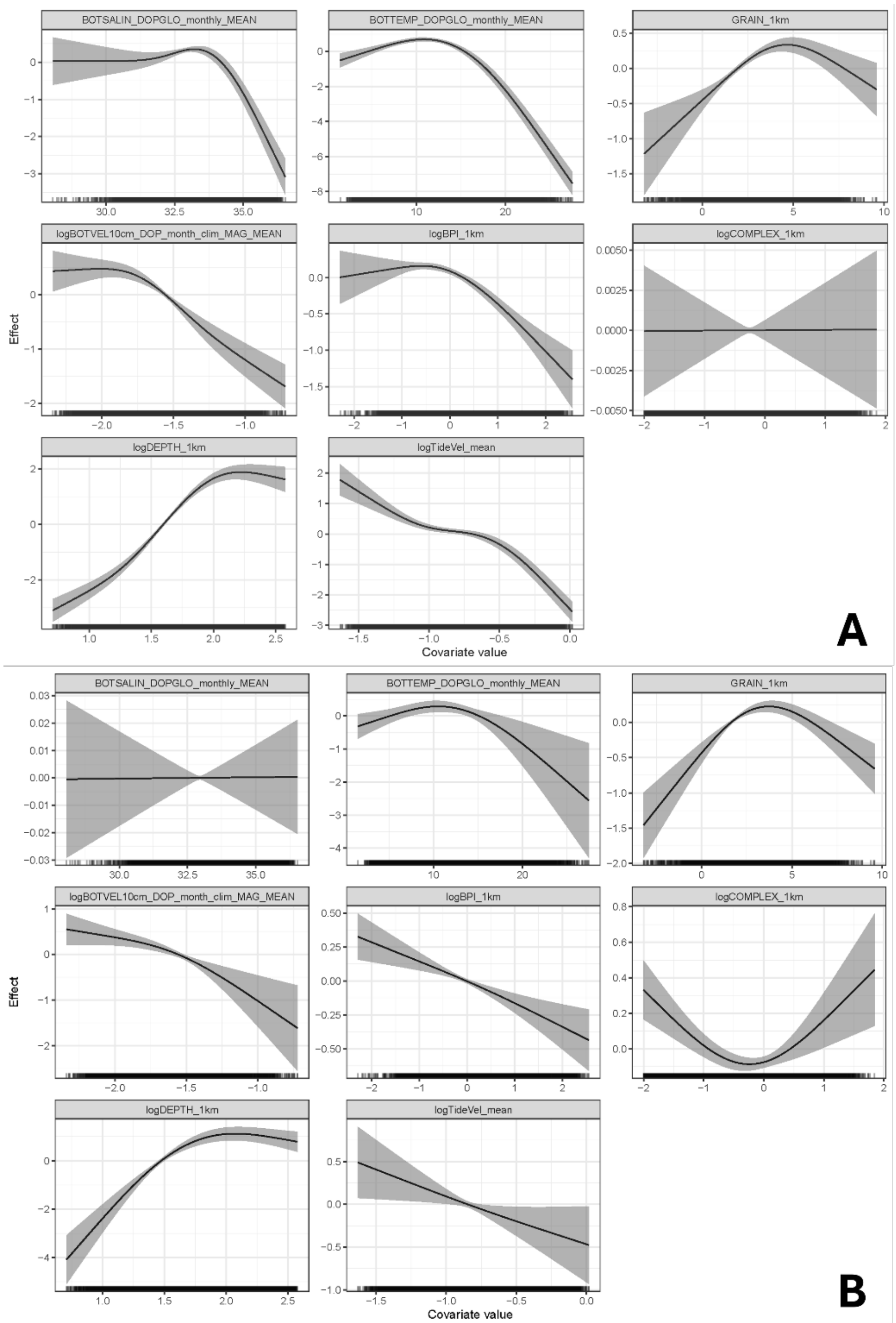

Figure 10. Smooth terms graphs depicting relationships between species counts and individual environmental covariates for adult monkfish (*Lophius americanus*). (A) Presence-absence component. (B) Zero-truncated negative binomial component of the joint hurdle species distribution model.

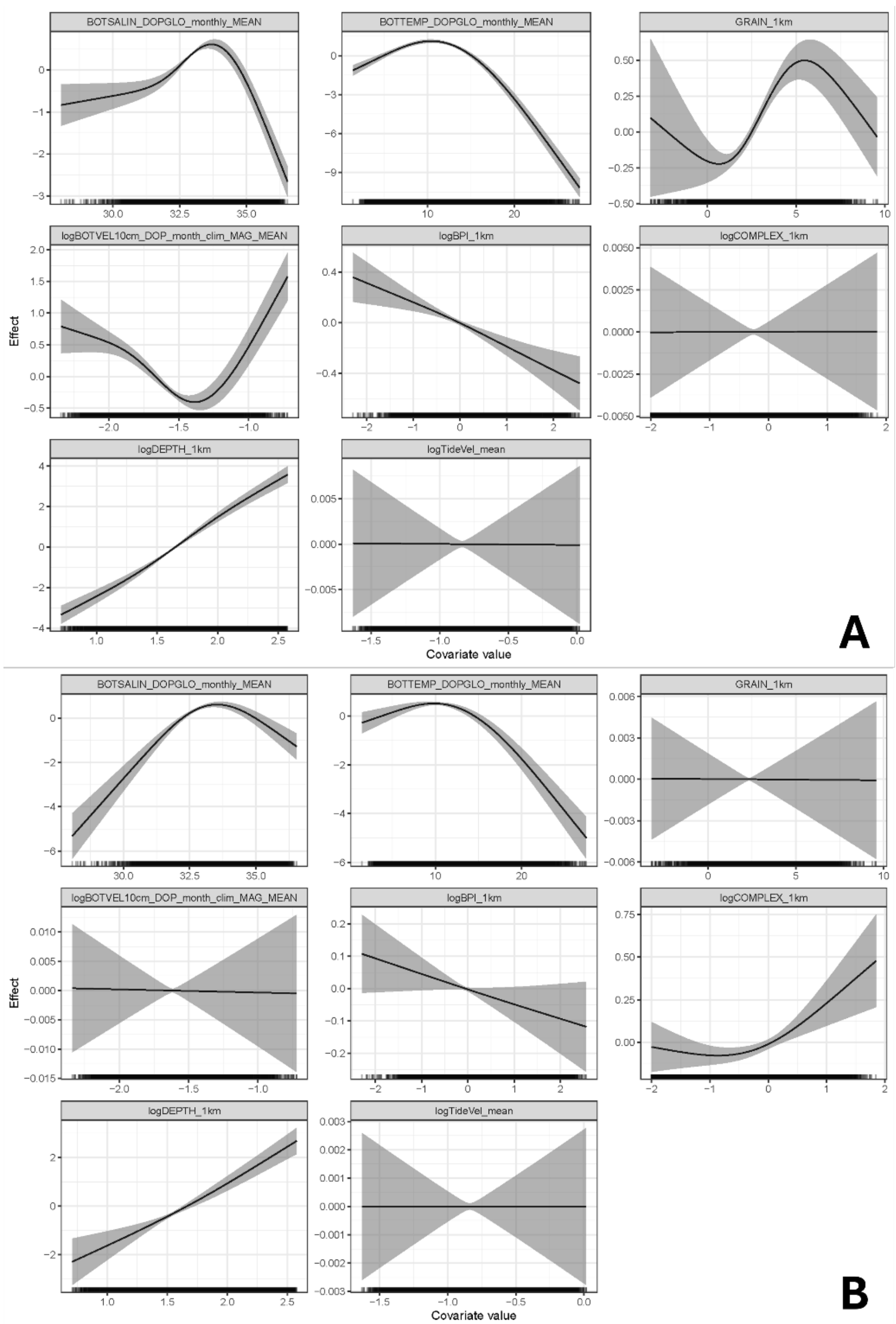

3.2.4 Barndoor skate

Figure 11. Smooth terms graphs depicting relationships between species counts and individual environmental covariates for pooled juvenile and adult barndoor skate (*Dipturus laevis*). (A) Presence-absence component. (B) Zero-truncated negative binomial component of the joint hurdle species distribution model.

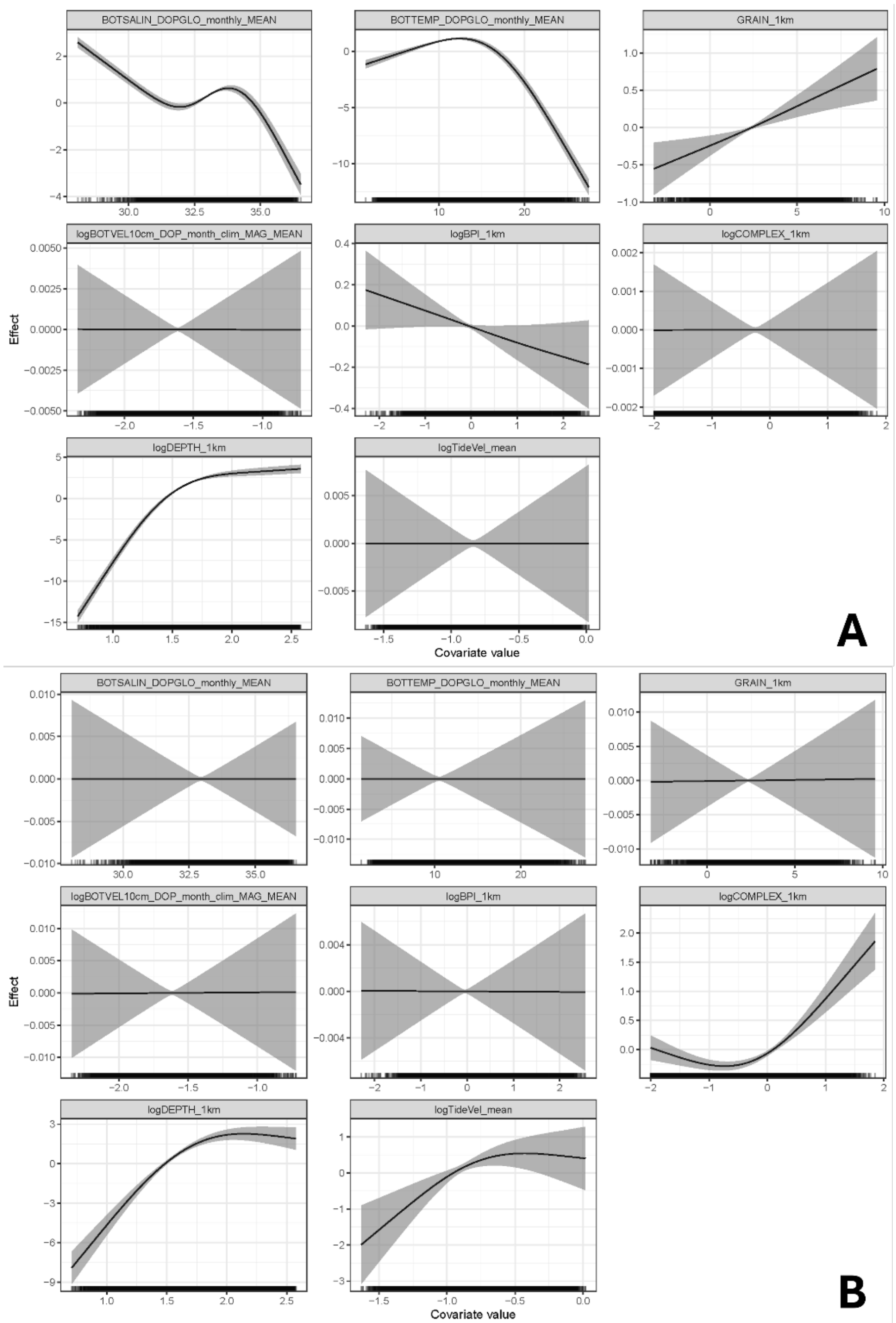

3.2.5 Clearnose skate

Figure 12. Smooth terms graphs depicting relationships between species counts and individual environmental covariates for juvenile clearnose skate (*Rostroraja eglanteria*). (A) Presence-absence component. (B) Zero-truncated negative binomial component of the joint hurdle species distribution model.

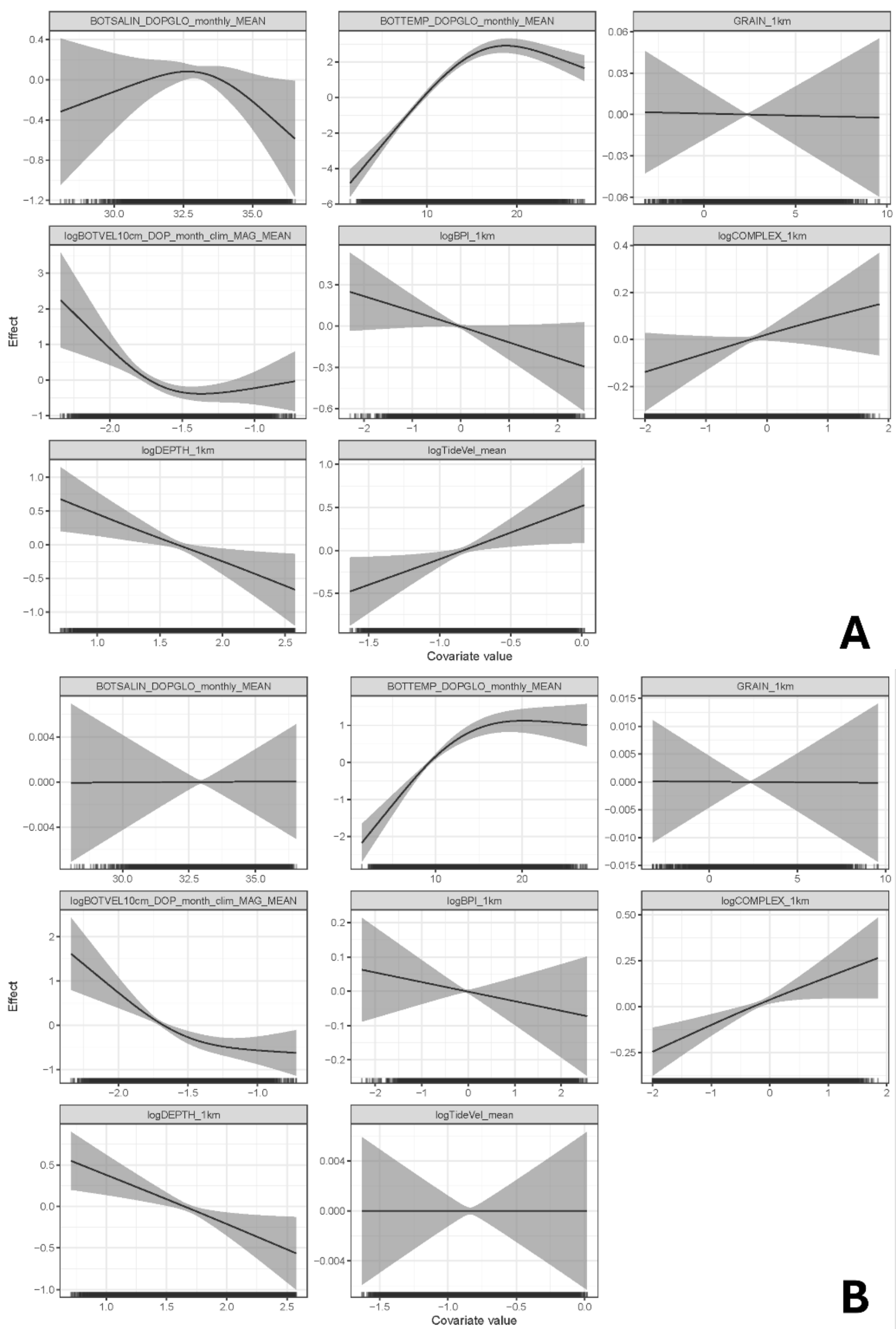

Figure 13. Smooth terms graphs depicting relationships between species counts and individual environmental covariates for adult clearnose skate (*Rostroraja eglanteria*). (A) Presence-absence component. (B) Zero-truncated negative binomial component of the joint hurdle species distribution model.

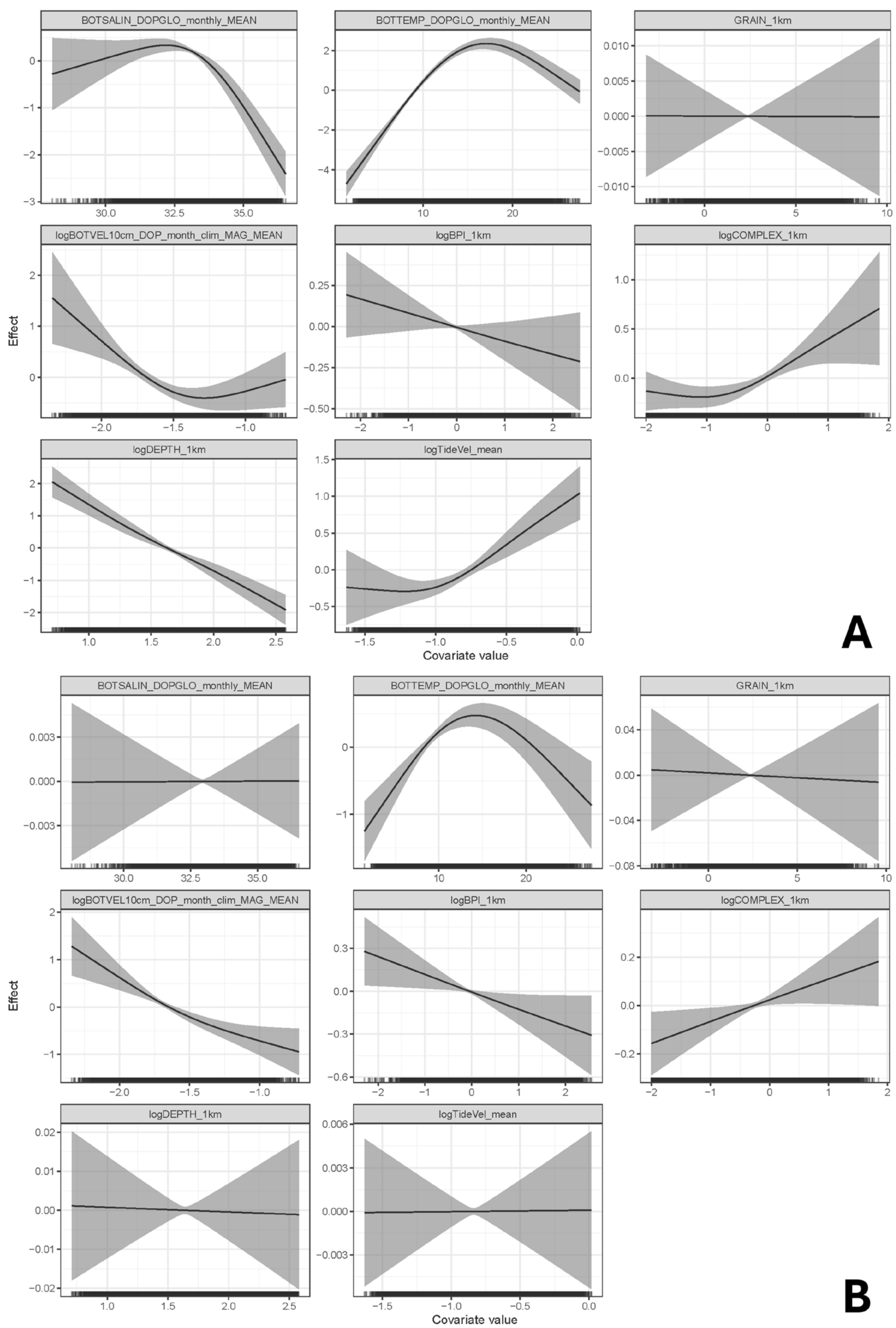

3.2.6 Little skate

Figure 14. Smooth terms graphs depicting relationships between species counts and individual environmental covariates for juvenile little skate (*Leucoraja erinacea*). (A) Presence-absence component. (B) Zero-truncated negative binomial component of the joint hurdle species distribution model.

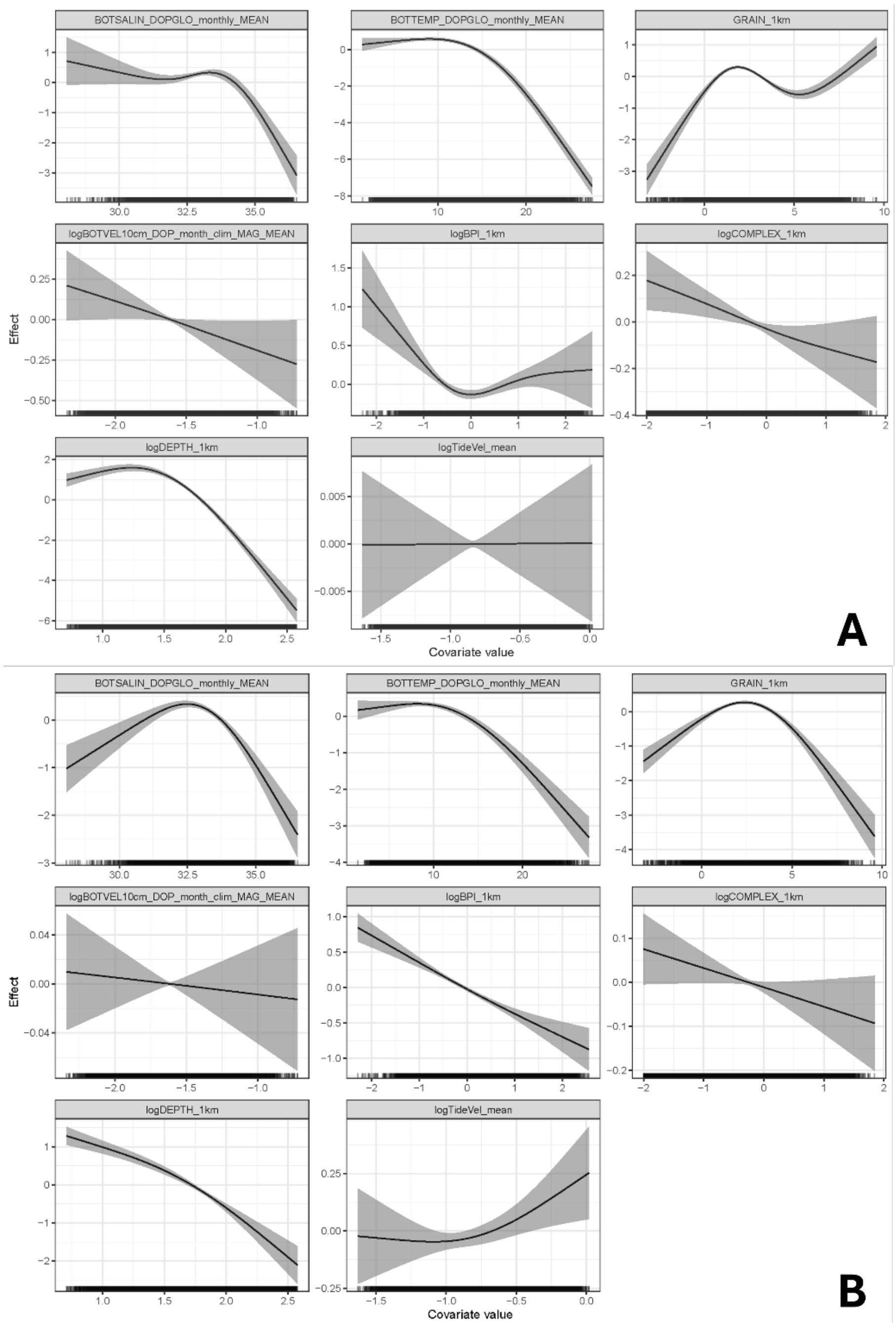

Figure 15. Smooth terms graphs depicting relationships between species counts and individual environmental covariates for adult little skate (*Leucoraja erinacea*). (A) Presence-absence component. (B) Zero-truncated negative binomial component of the joint hurdle species distribution model.

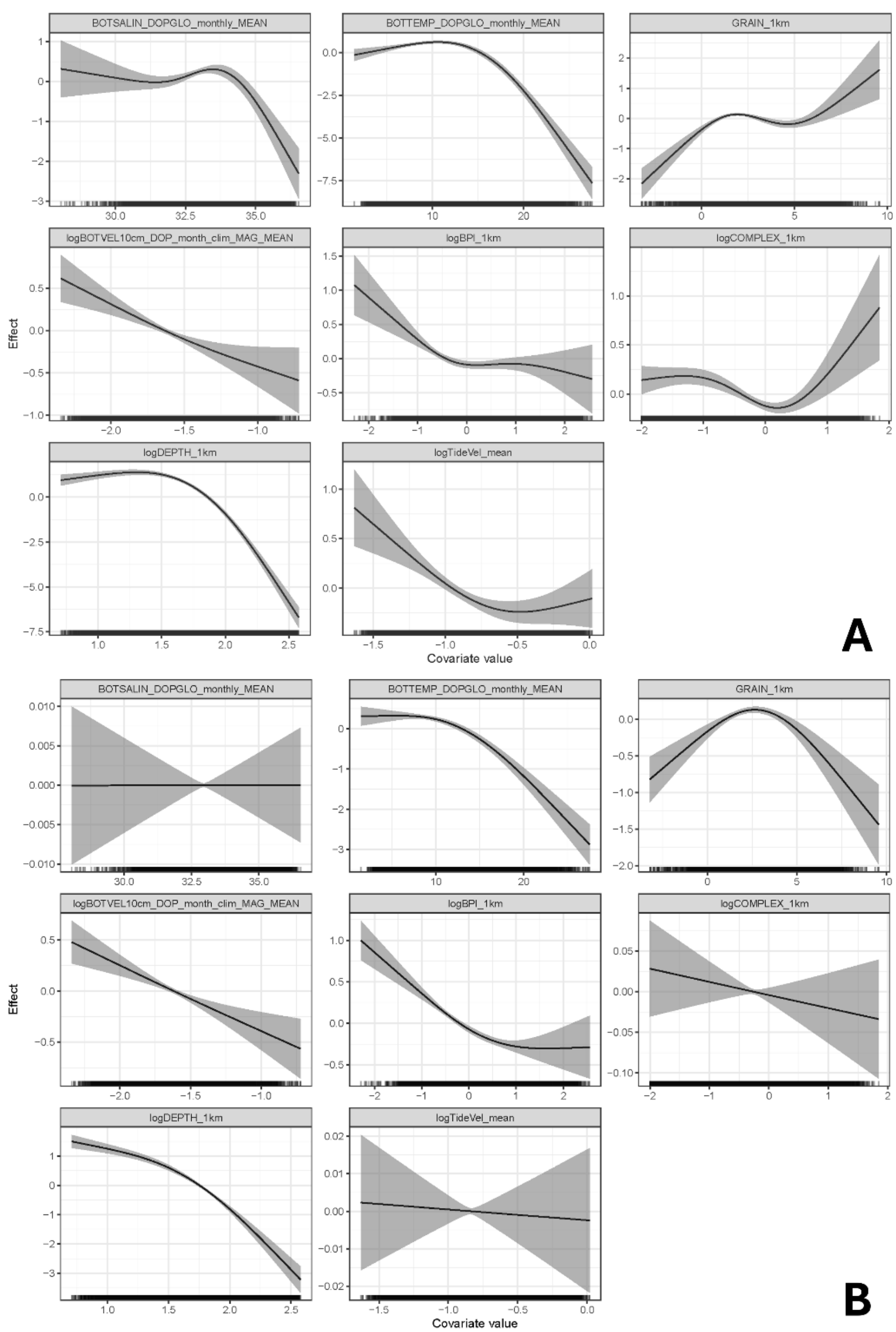

3.2.7 Rosette skate

Figure 16. Smooth terms graphs depicting relationships between species counts and individual environmental covariates for pooled juvenile and adult rosette skate (*Leucoraja garmani*). (A) Presence-absence component. (B) Zero-truncated negative binomial component of the joint hurdle species distribution model.

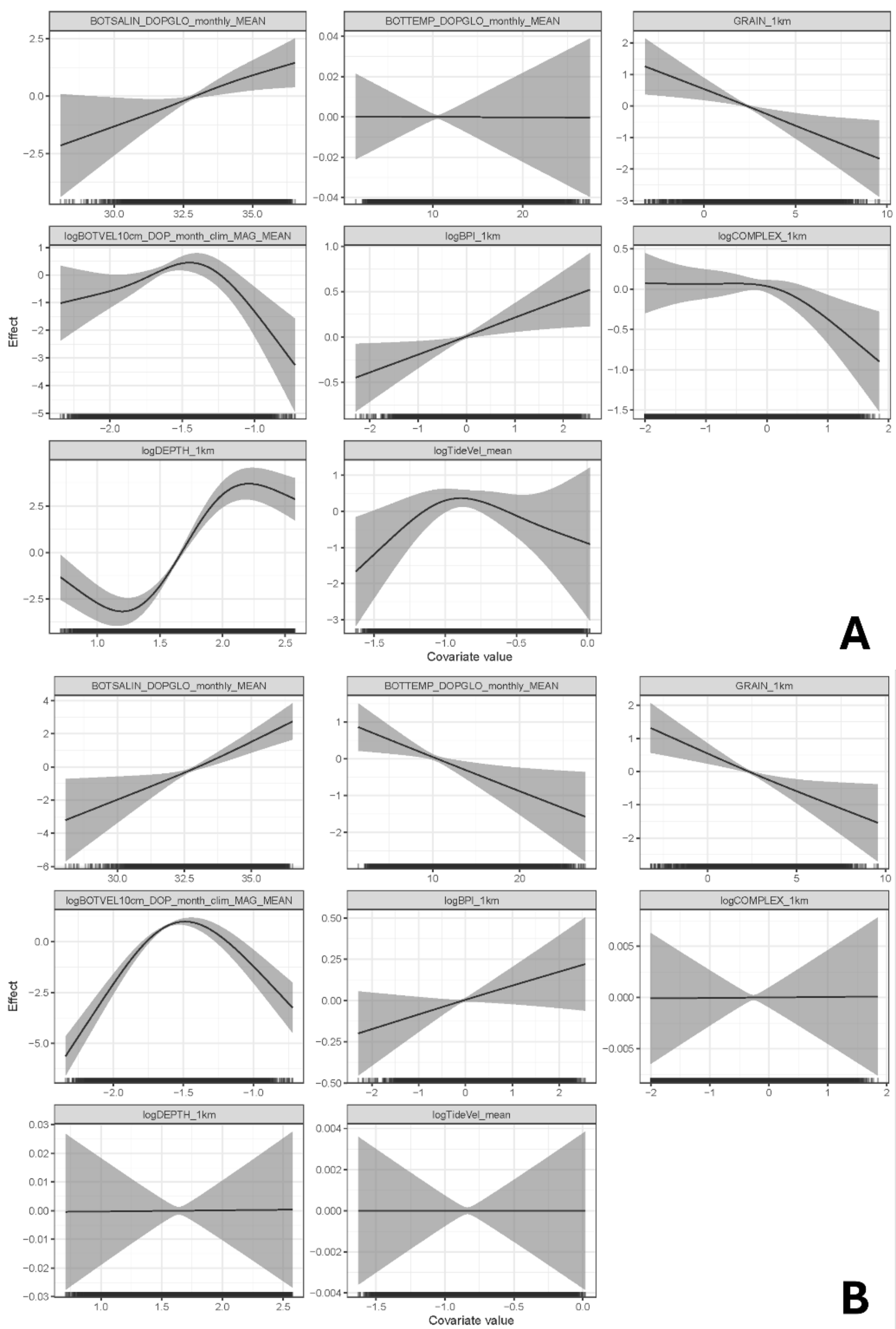

3.2.8 Smooth skate

Figure 17. Smooth terms graphs depicting relationships between species counts and individual environmental covariates for pooled juvenile and adult smooth skate (*Malacoraja senta*). (A) Presence-absence component. (B) Zero-truncated negative binomial component of the joint hurdle species distribution model.

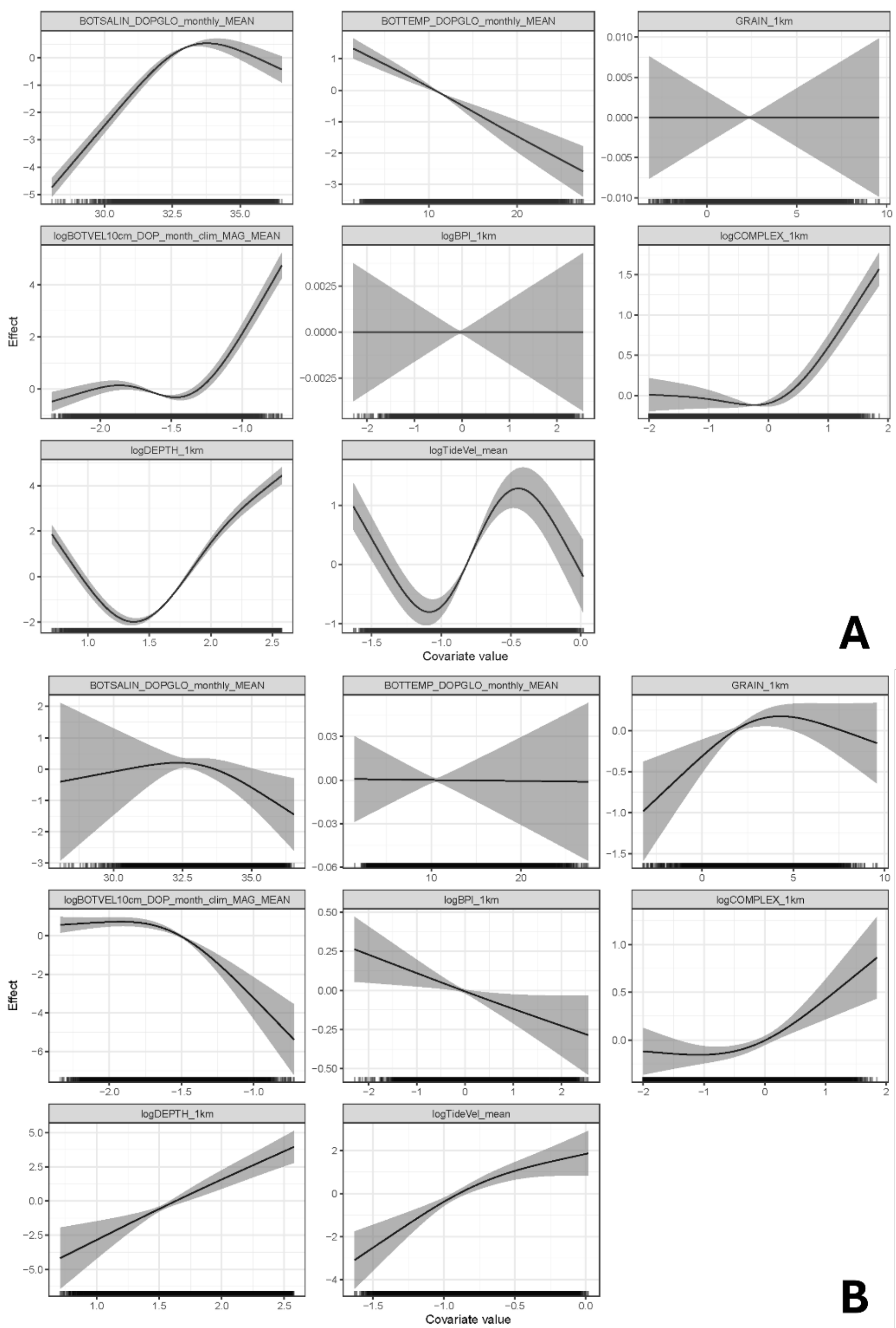

3.2.9 Thorny skate

Figure 18. Smooth terms graphs depicting relationships between species counts and individual environmental covariates for pooled juvenile and adult thorny skate (*Amblyraja radiata*). (A) Presence-absence component. (B) Zero-truncated negative binomial component of the joint hurdle species distribution model.

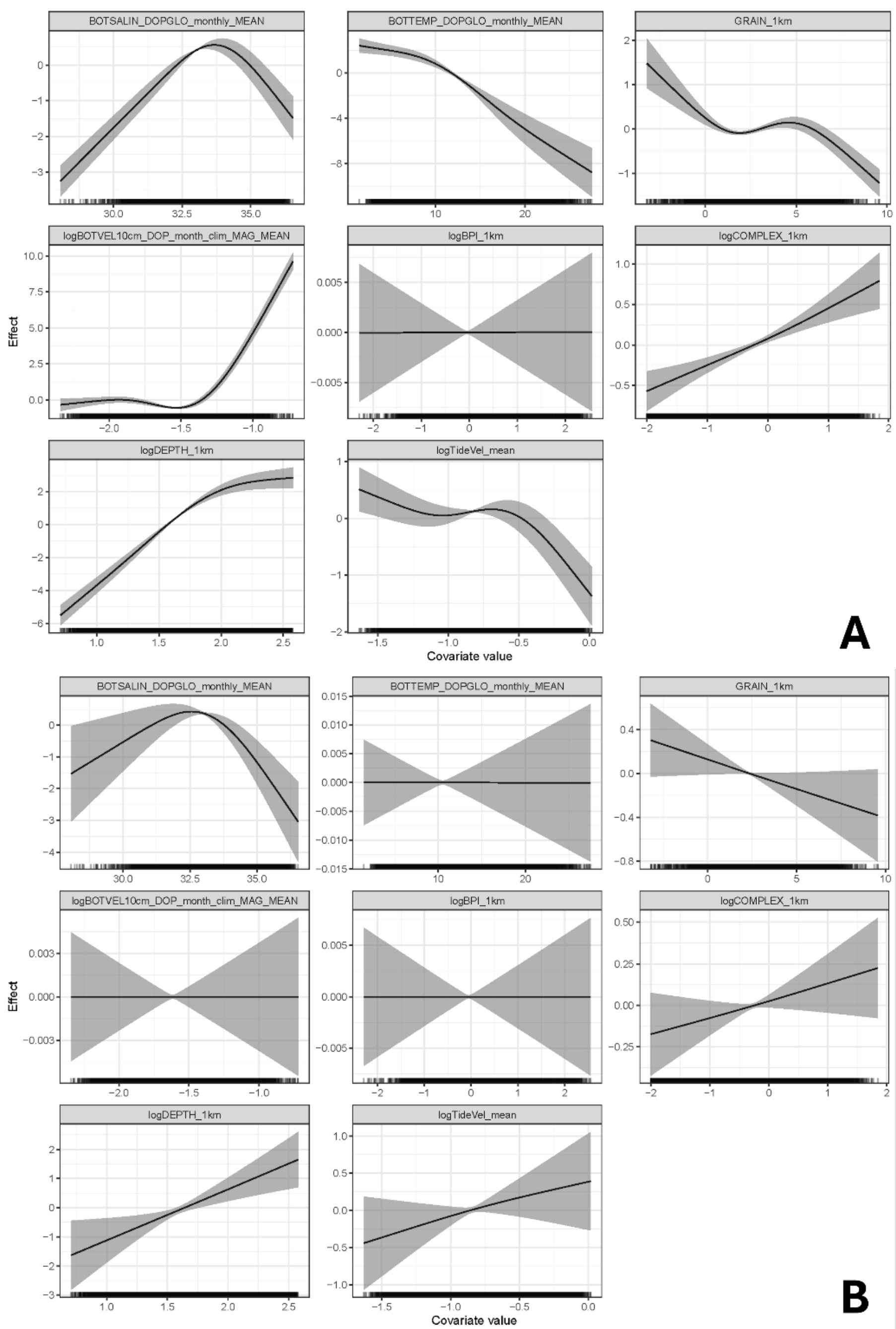

3.2.10 Winter skate

Figure 19. Smooth terms graphs depicting relationships between species counts and individual environmental covariates for juvenile winter skate (*Leucoraja ocellata*). (A) Presence-absence component. (B) Zero-truncated negative binomial component of the joint hurdle species distribution model.

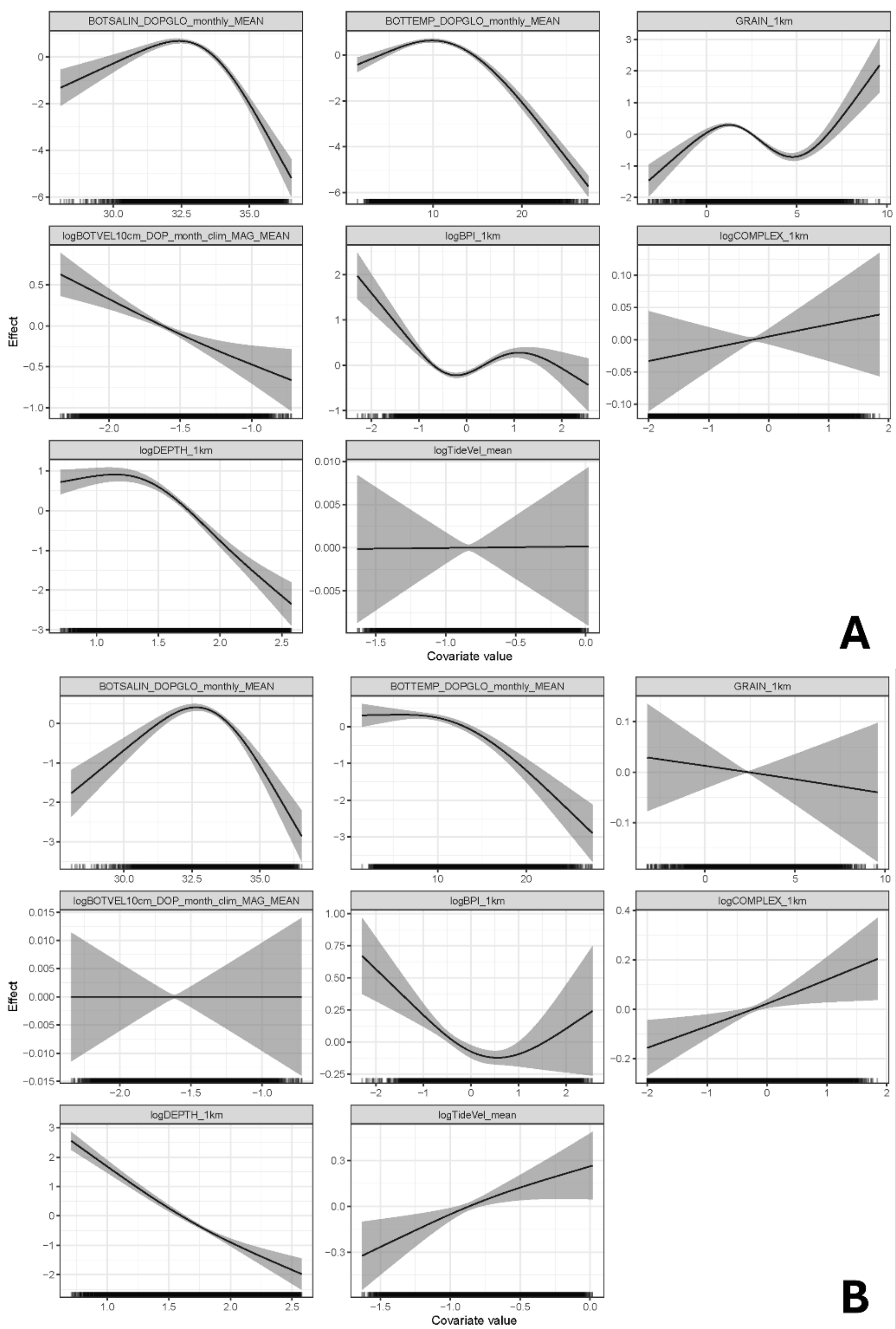

Figure 20. Smooth terms graphs depicting relationships between species counts and individual environmental covariates for adult winter skate (*Leucoraja ocellata*). (A) Presence-absence component. (B) Zero-truncated negative binomial component of the joint hurdle species distribution model.

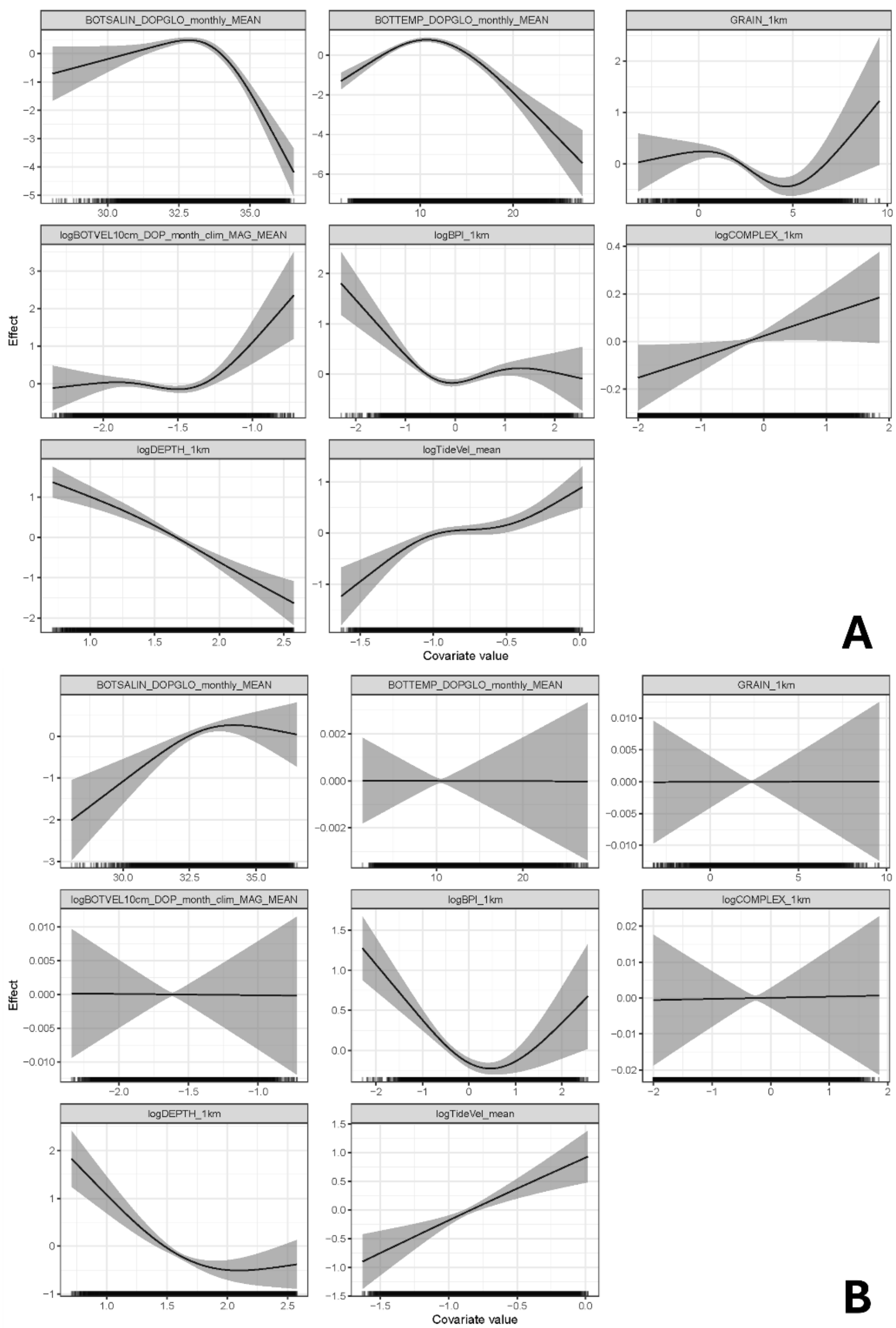

4.0 SPATIAL DISTRIBUTION

In this section, we have included species-specific spatial distribution outputs that complement the updated EFH designation maps. As noted in the Framework document and Appendix E: Detailed EFH Methods, the EFH maps are based on predicted densities from the models, combined with inshore data. Generally, the model outputs are the most important element of the EFH maps given the large extent of the model domain and the inclusion of both inshore and offshore survey data in the models. Inshore fish survey data add estuarine and coastal areas to the EFH maps beyond what is reflected in the maps in this section. Thus, the EFH designation maps may appear different from the plots in this appendix, especially for species that occur in larger numbers inshore.

For each species, both quantile and continuous density plots are shown. First, we show predicted density as four quantiles. The 25%, 50%, and 75% quantiles (yellow, green, and blue) are combined to form the basis of the EFH map, and the 95% quantile (purple) reflects lower density areas. Areas with the lowest 5% of predicted density are not shown. We also provide actual model estimated densities, mapped using a continuous purple to red color ramp. Note that the scale of these continuous maps varies by species (i.e., the redder colors may represent dozens or hundreds of fish per grid cell, depending on the plot).

The densities mapped here reflect a mean/maximum approach. All plots were developed by first calculating the mean density value in each model grid cell across 22 years and then selecting the maximum mean density value across all months or a seasonal subset of months. The larger left-hand panels show the maximum mean value across all six months (March, April, May, September, October, November), and the seasonal spring and fall panels on the upper and lower right-hand side show the maximum mean for spring (March-May) or fall (September-November), respectively. As noted in Appendix E, maximum values within the year are used to provide a conservative estimate of where a species and life stage might be abundant across the seasons. While the six-month plots are generally the basis for the EFH maps, the seasonal products are shown here to reflect the sometimes notable differences in distribution between spring and fall, which may be important for EFH consultation or other applications.

4.1 ATLANTIC COD

Figure 21. 22-year maximum predicted density (species counts) quantiles for juvenile Atlantic cod (*Gadus morhua*). Maps depict the maximum of the 22-year averages across (A) the full temporal range of the model (six months); and (C) fall survey months (September-November).

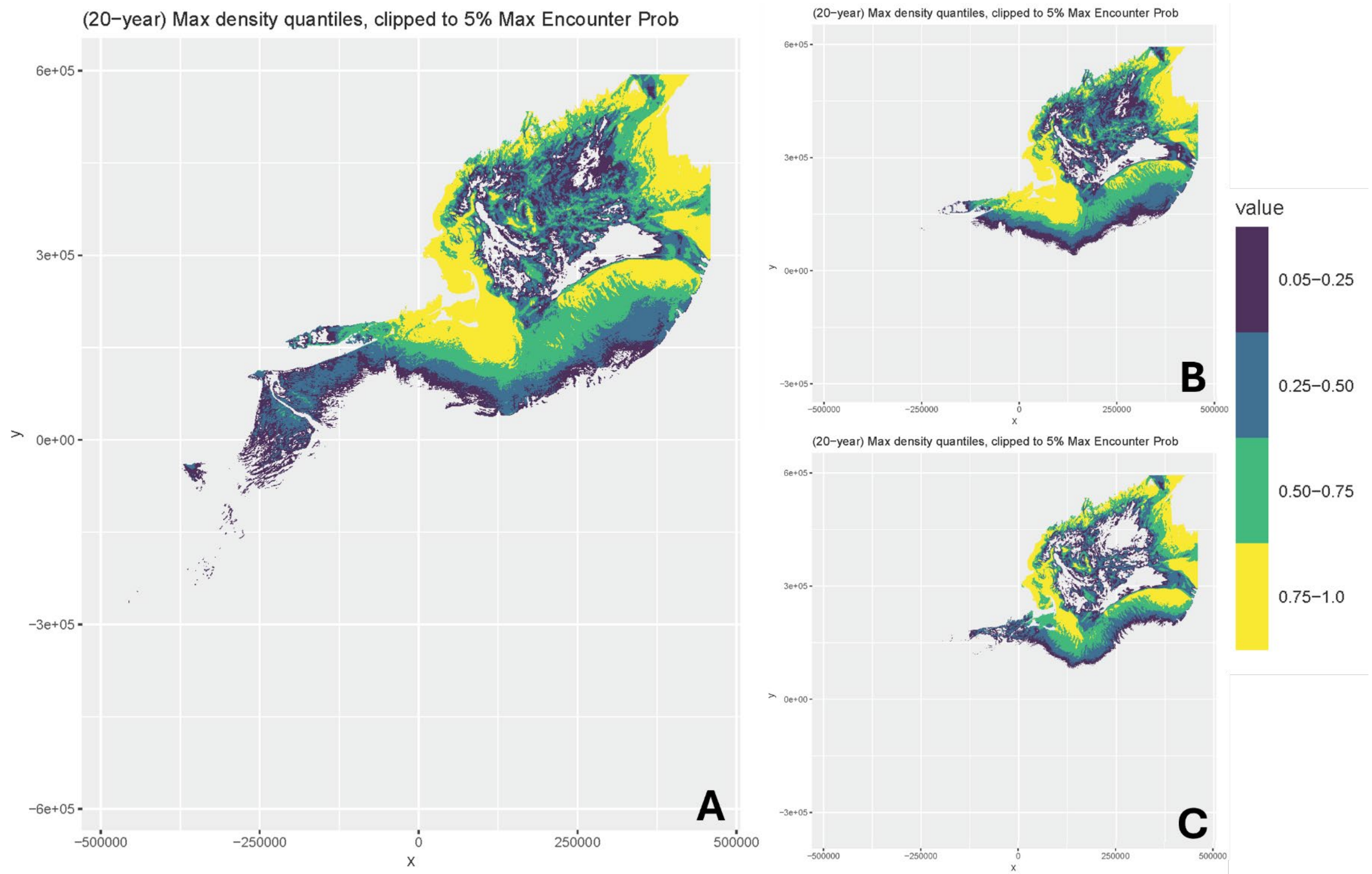

Figure 22. 22-year mean predicted density (species counts) for juvenile Atlantic cod (*Gadus morhua*). Maps depict the maximum of the 22-year averages across (A) the full temporal range of the model (six months); (B) spring survey months (March-May); and (C) fall survey months (September-November).

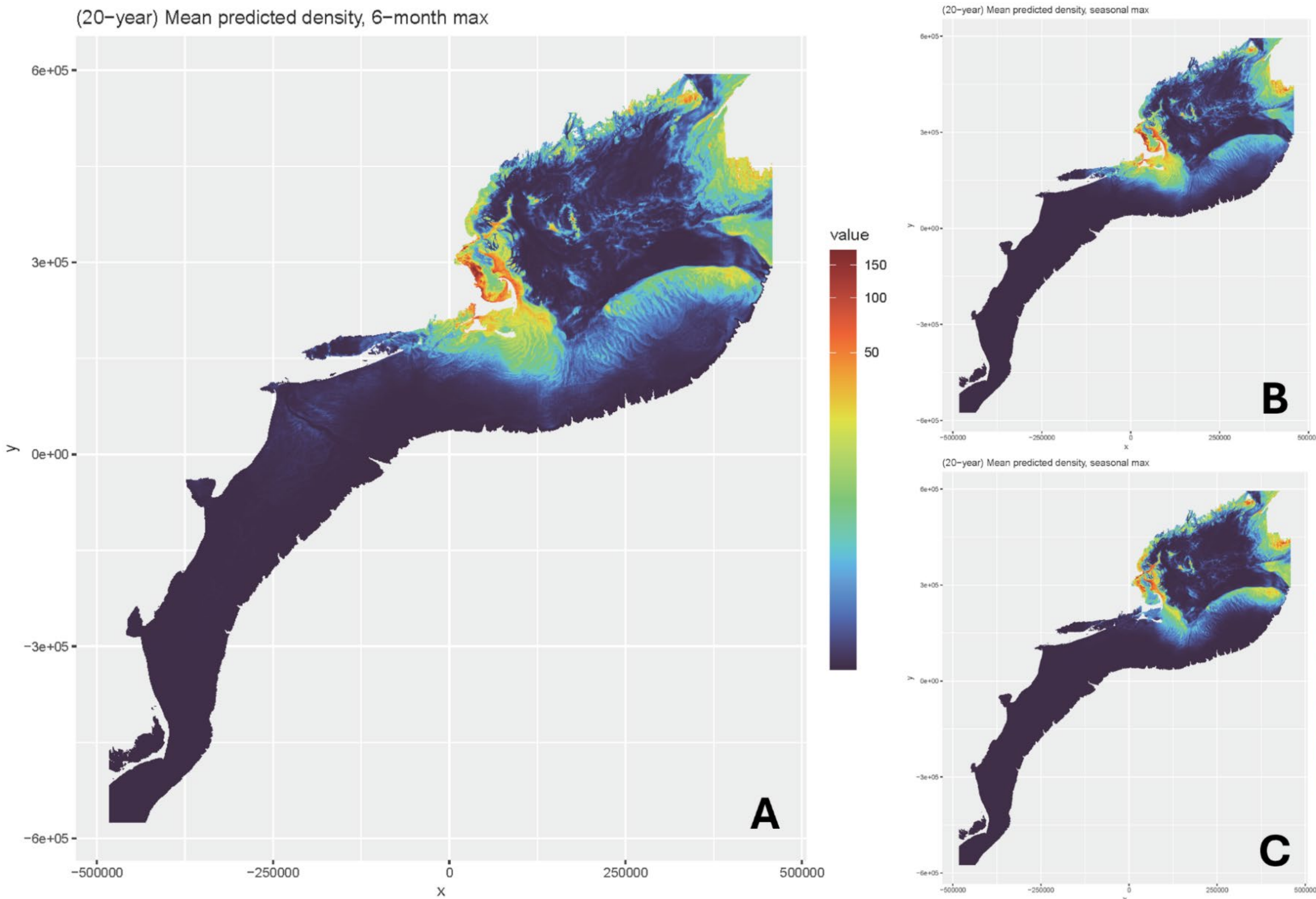

Figure 23. 22-year maximum predicted density (species counts) quantiles for adult Atlantic cod (*Gadus morhua*). Maps depict the maximum of the 22-year averages across (A) the full temporal range of the model (six months); and (C) fall survey months (September-November).

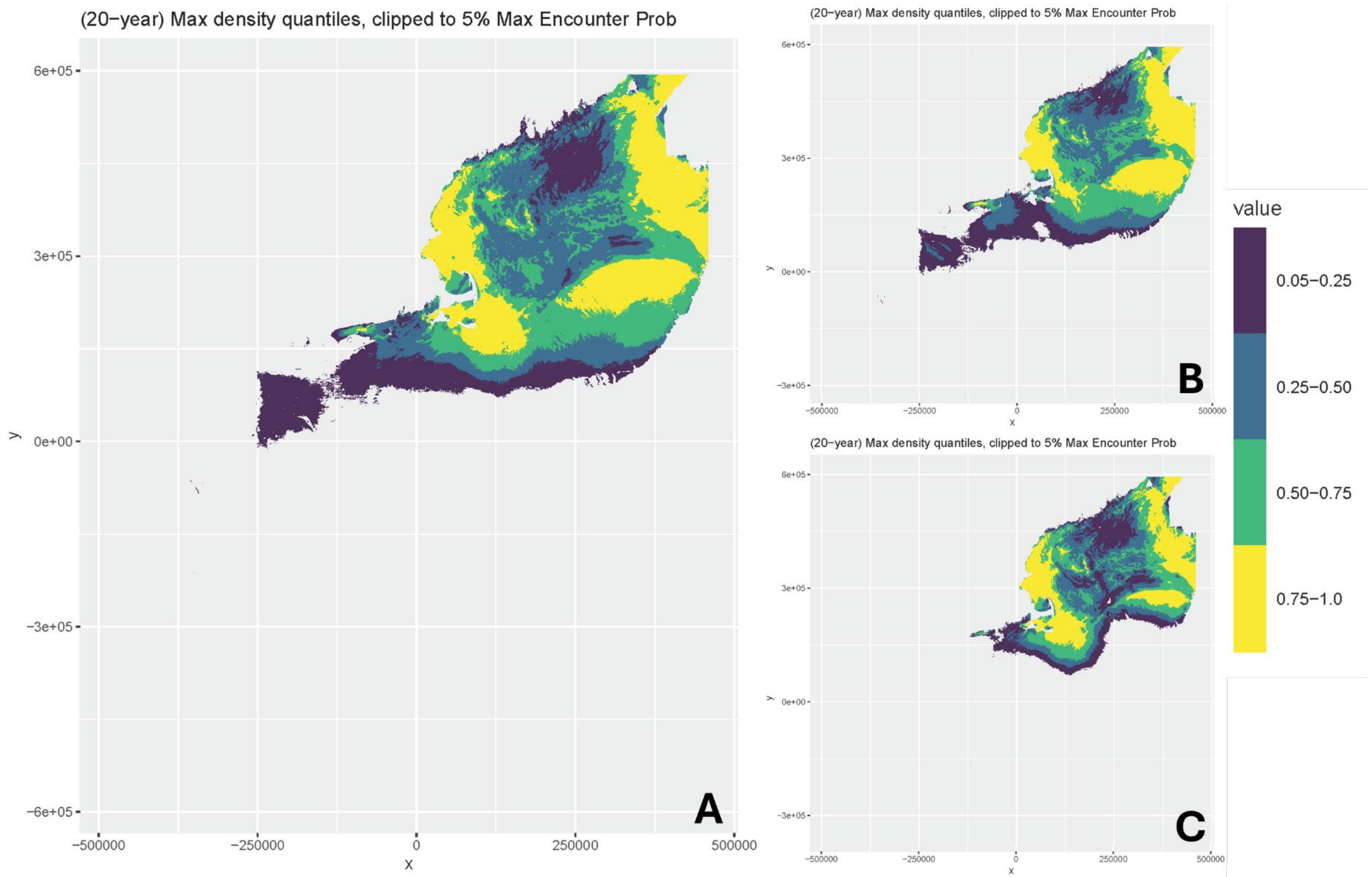

Figure 24. 22-year mean predicted density (species counts) for adult Atlantic cod (*Gadus morhua*). Maps depict the maximum of the 22-year averages across (A) the full temporal range of the model (six months); and (C) fall survey months (September-November).

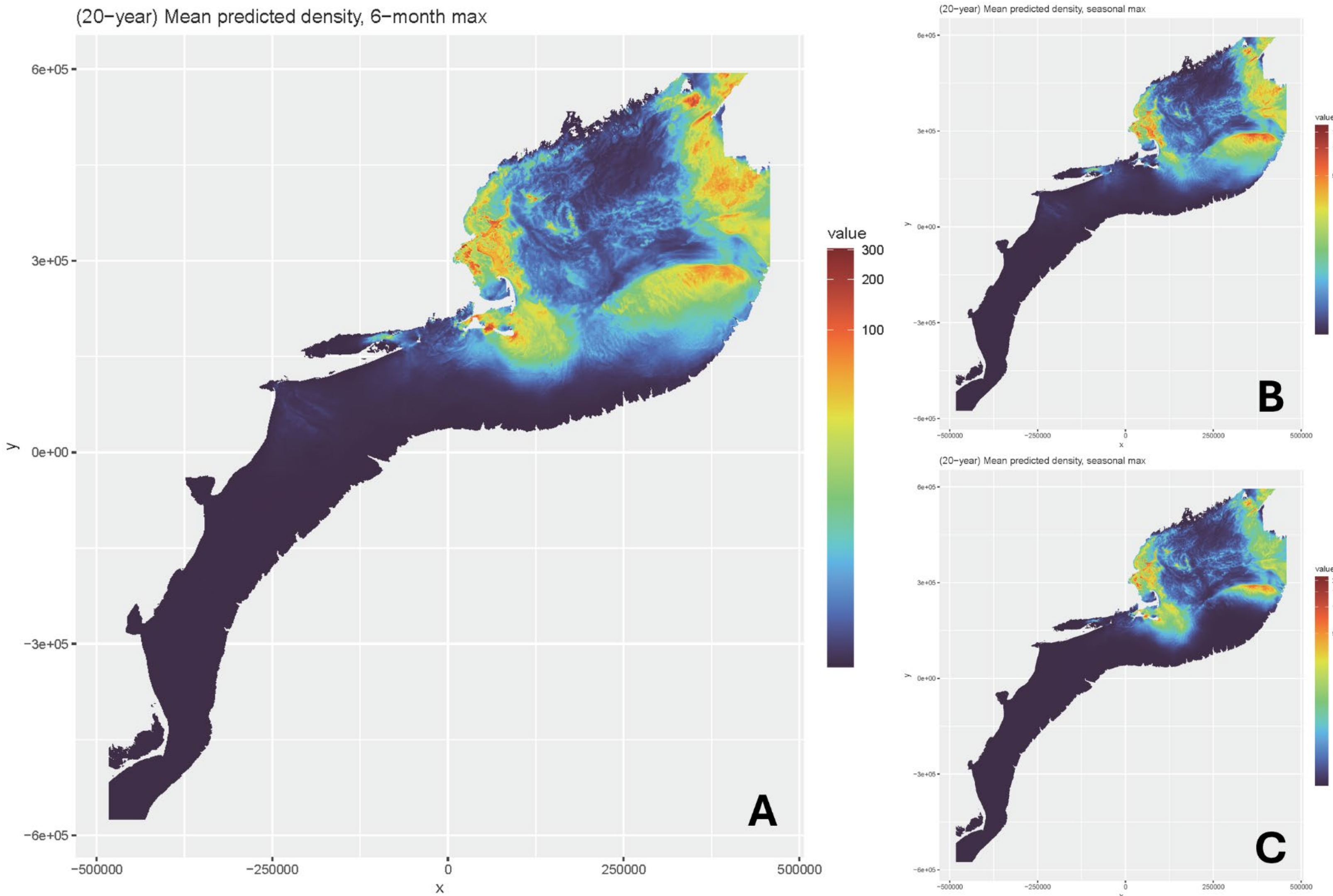

4.2 ATLANTIC HERRING

Figure 25. 22-year maximum predicted density (species counts) quantiles for juvenile Atlantic herring (*Clupea harengus*). Maps depict the maximum of the 22-year averages across (A) the full temporal range of the model (six months); and (C) fall survey months (September-November).

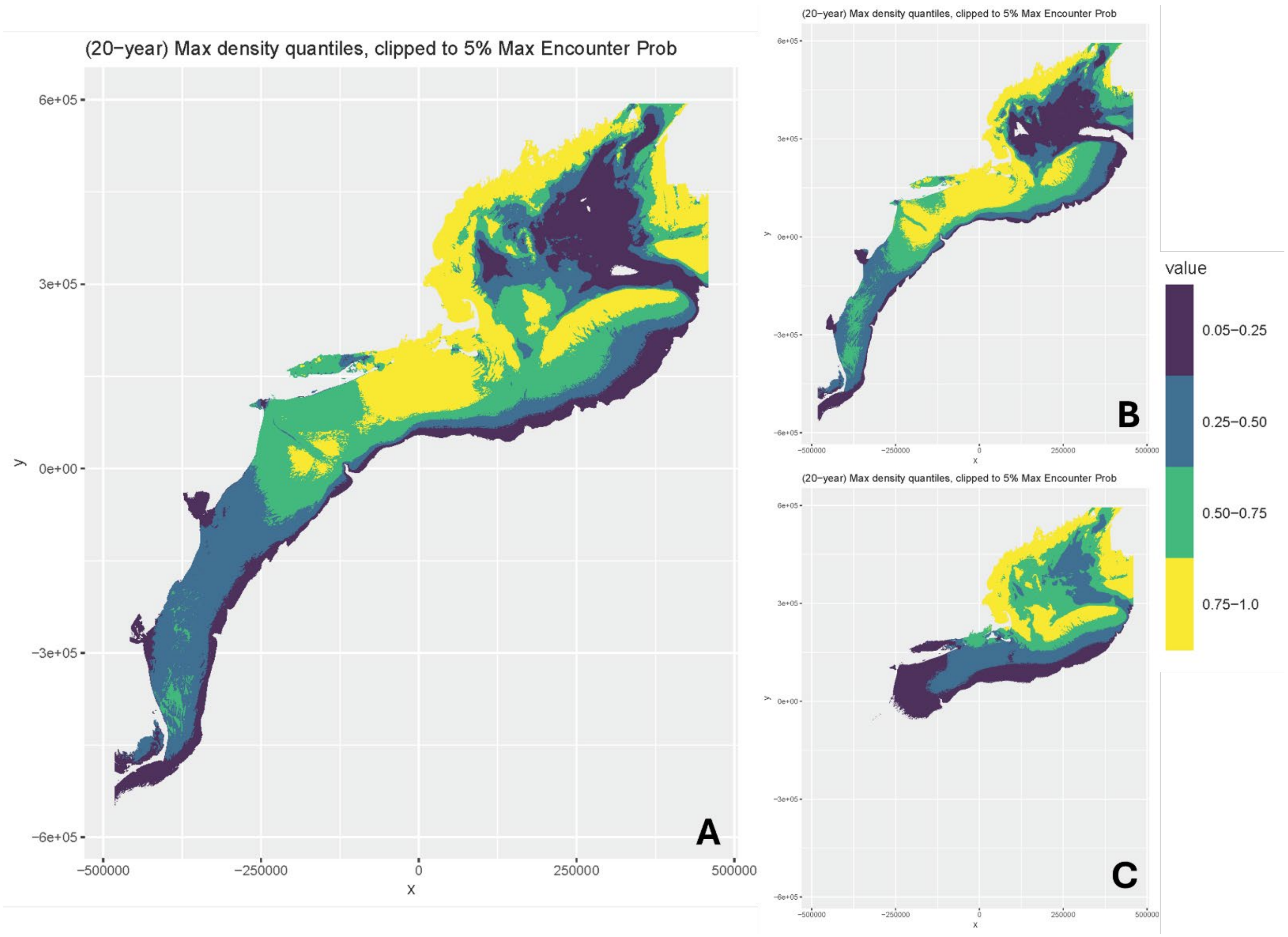

Figure 26. 22-year mean predicted density (species counts) for juvenile Atlantic herring (*Clupea harengus*). Maps depict the maximum of the 22-year averages across (A) the full temporal range of the model (six months); and (C) fall survey months (September-November).

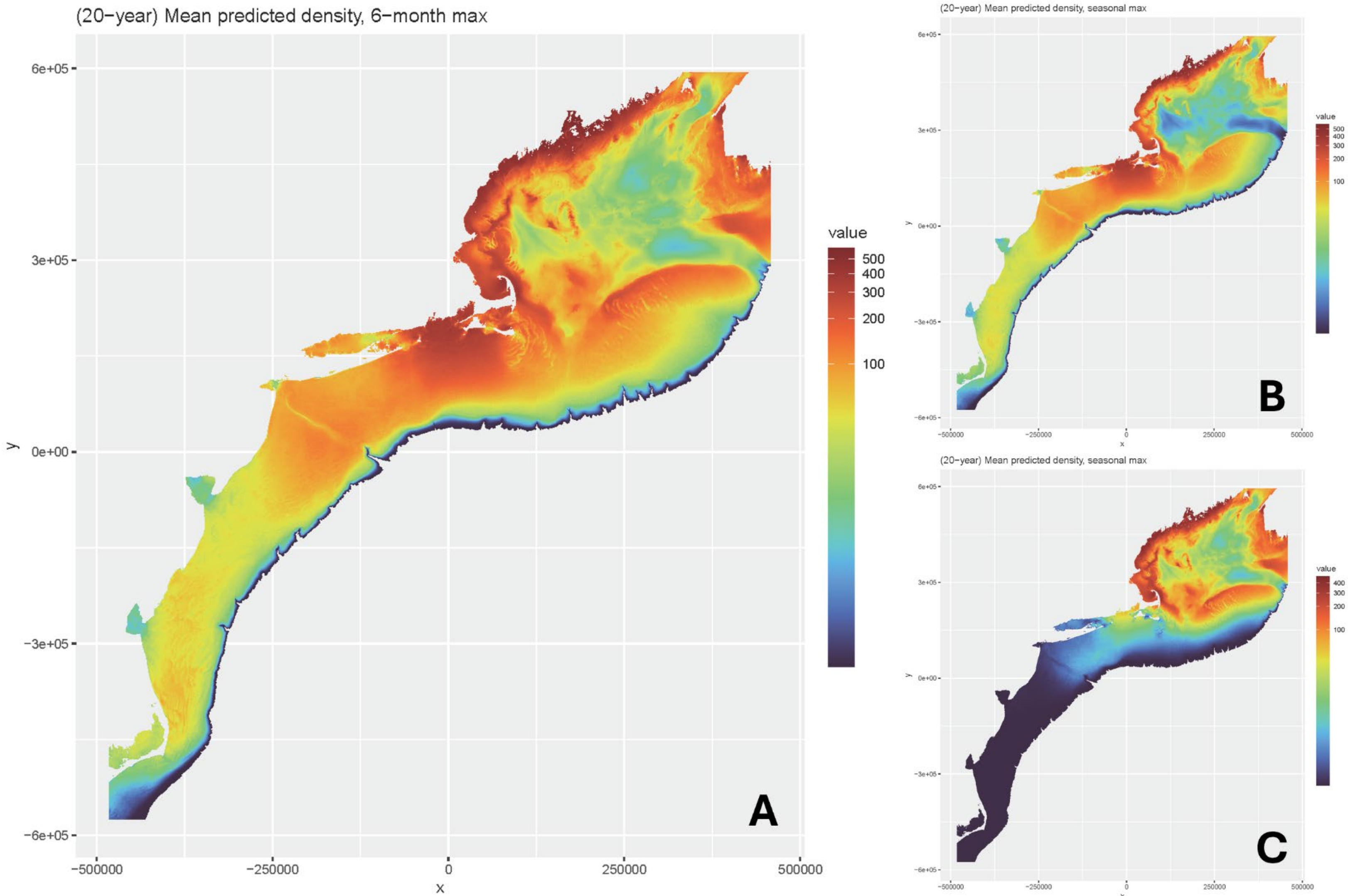

Figure 27. 22-year maximum predicted density (species counts) quantiles for adult Atlantic herring (*Clupea harengus*). Maps depict the maximum of the 22-year averages across (A) the full temporal range of the model (six months); and (C) fall survey months (September-November).

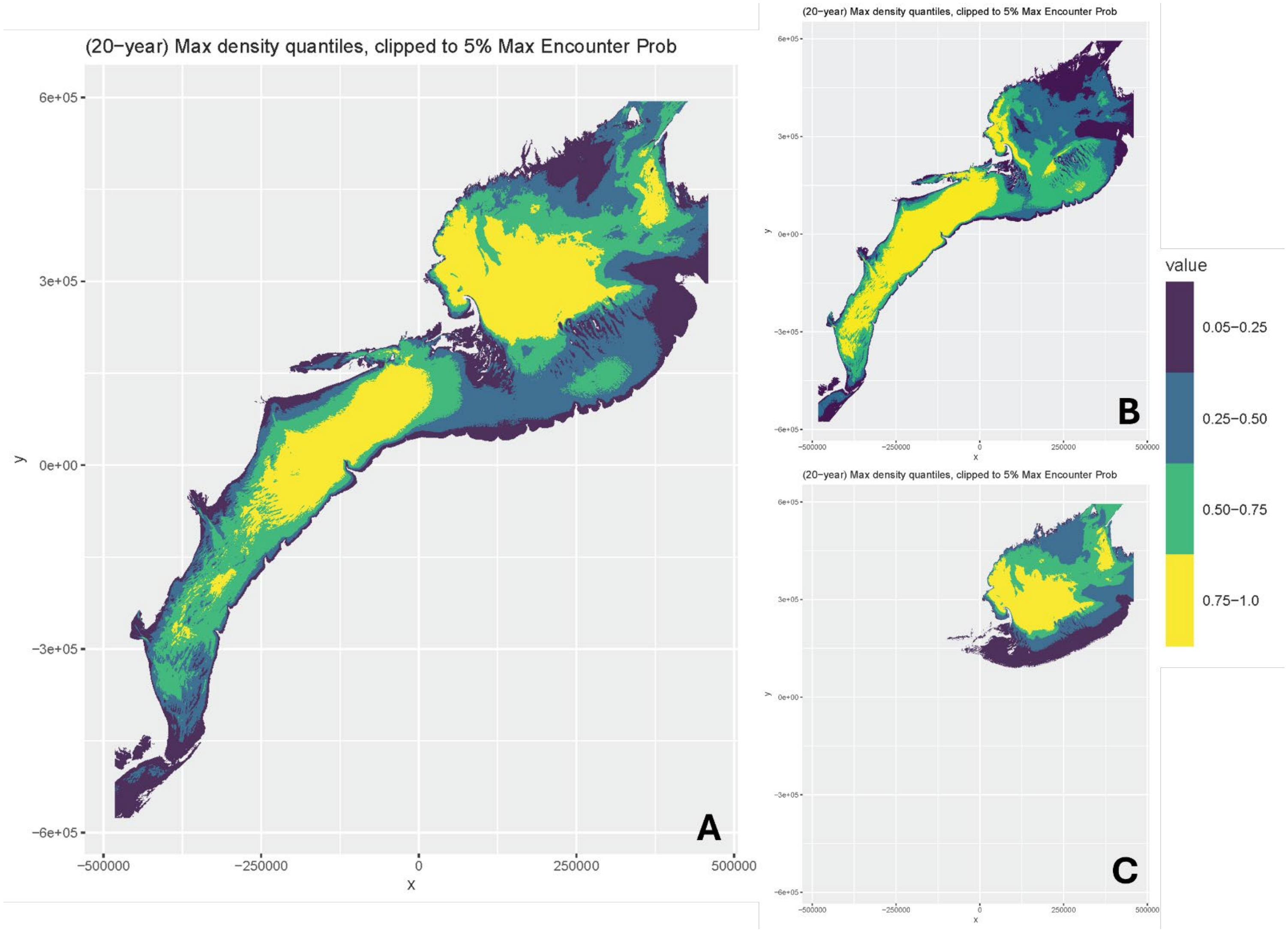

Figure 28. 22-year mean predicted density (species counts) for adult Atlantic herring (*Clupea harengus*). Maps depict the maximum of the 22-year averages across (A) the full temporal range of the model (six months); and (C) fall survey months (September-November).

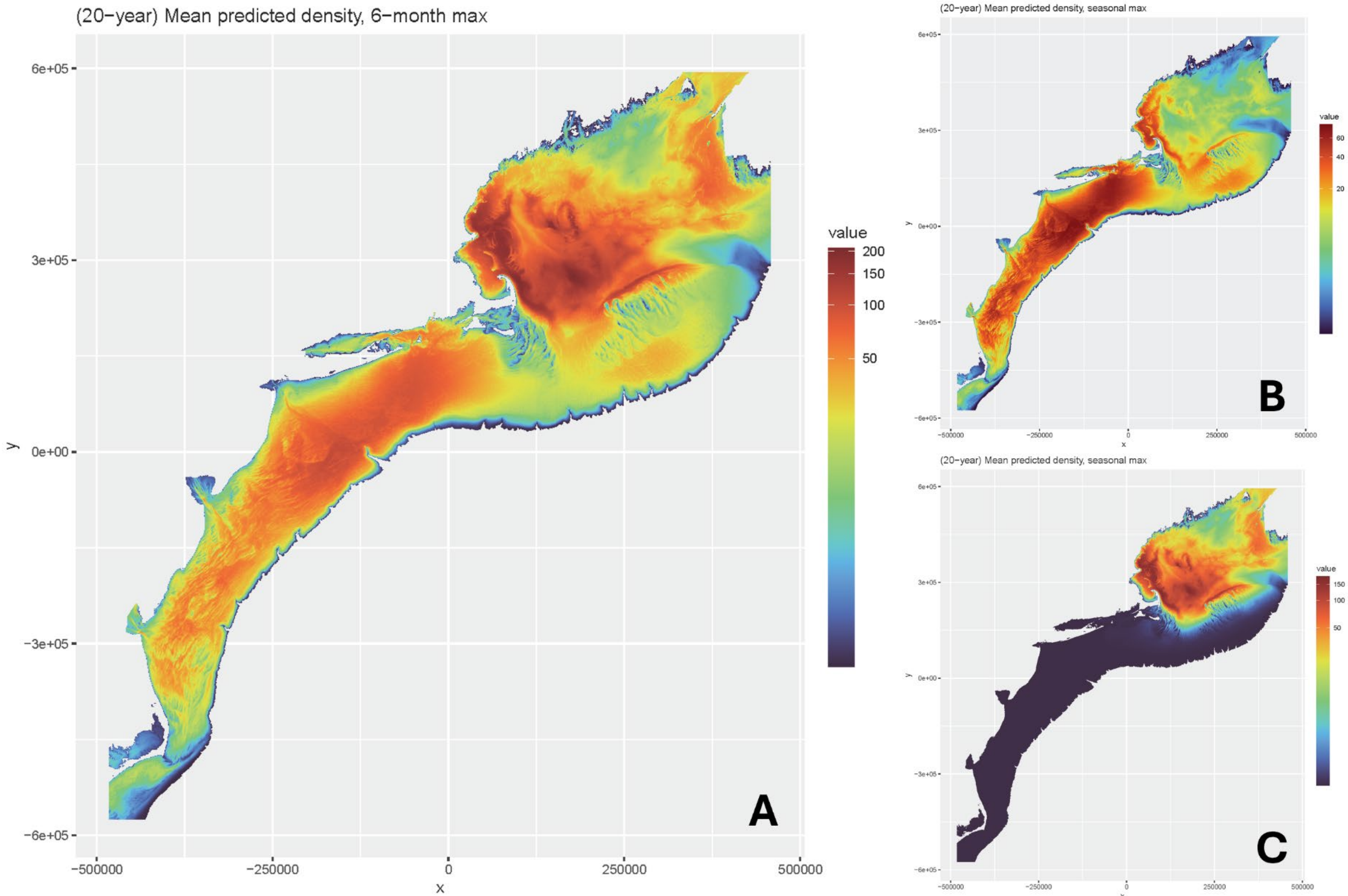

4.3 MONKFISH

Figure 29. 22-year maximum predicted density (species counts) quantiles for juvenile monkfish (*Lophius americanus*). Maps depict the maximum of the 22-year averages across (A) the full temporal range of the model (six months); and (C) fall survey months (September-November).

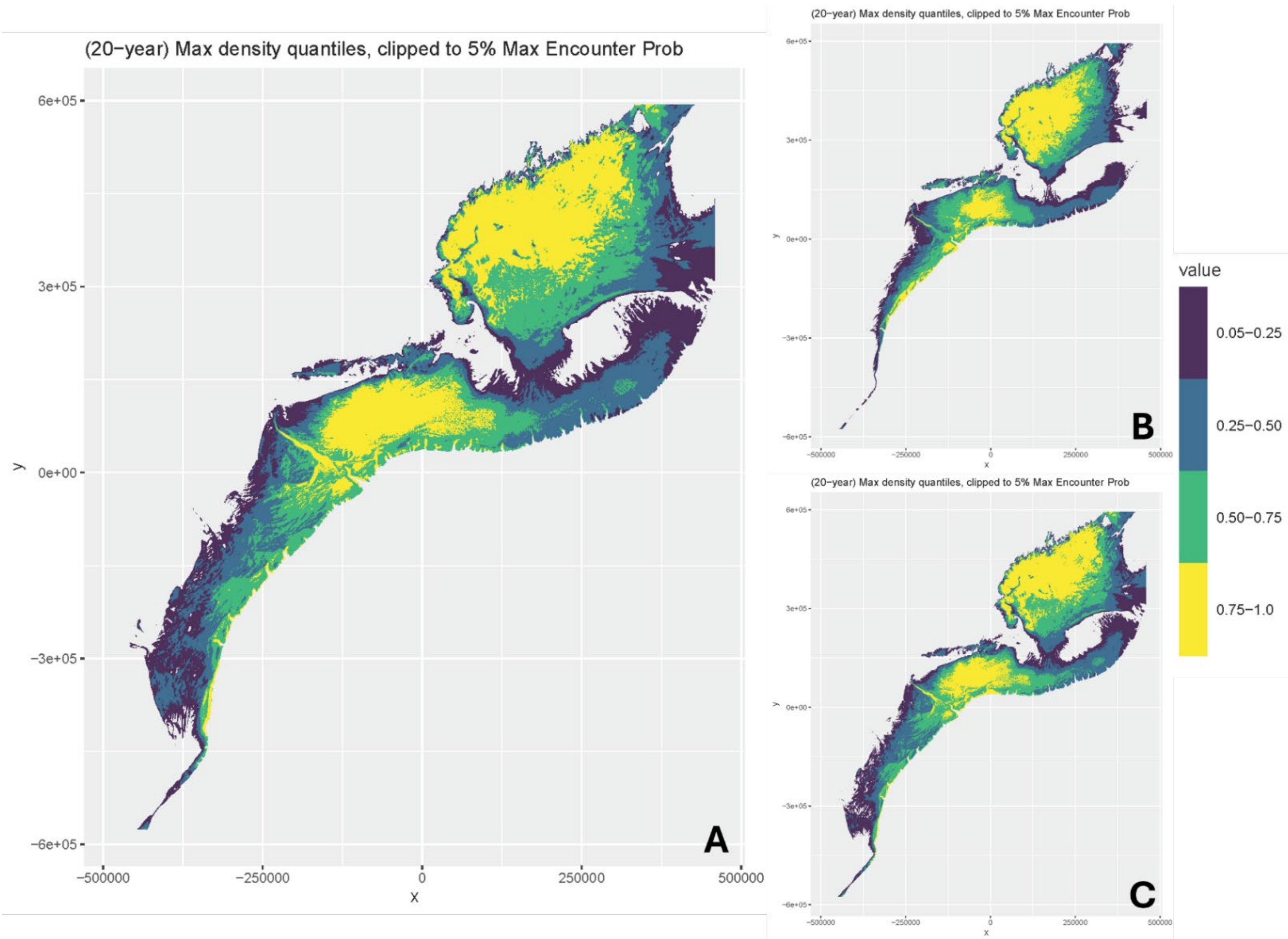

Figure 30. 22-year mean predicted density (species counts) for juvenile monkfish (*Lophius americanus*). Maps depict the maximum of the 22-year averages across (A) the full temporal range of the model (six months); and (C) fall survey months (September-November).

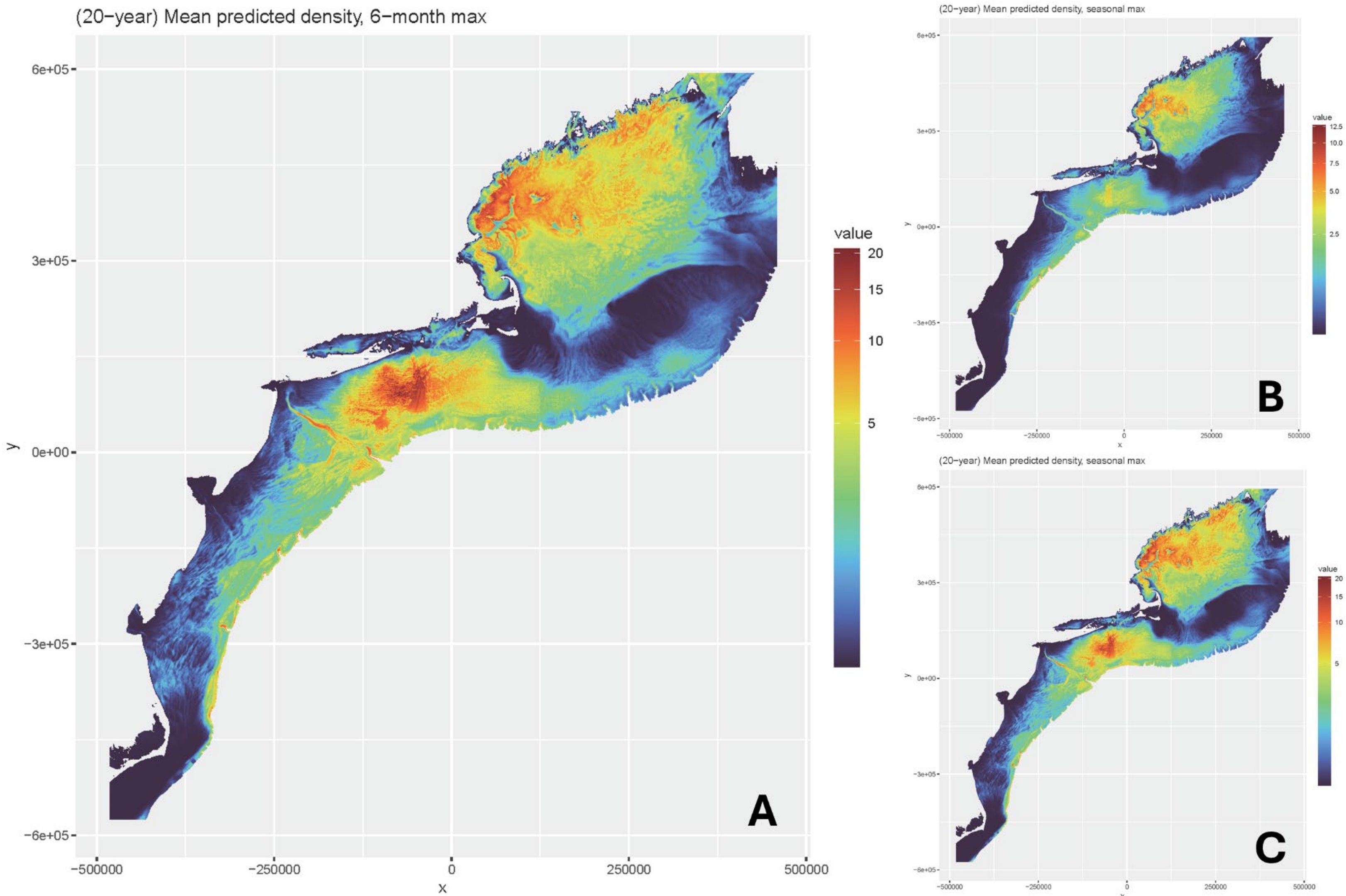

Figure 31. 22-year maximum predicted density (species counts) quantiles for adult monkfish (*Lophius americanus*). Maps depict the maximum of the 22-year averages across (A) the full temporal range of the model (six months); and (C) fall survey months (September-November).

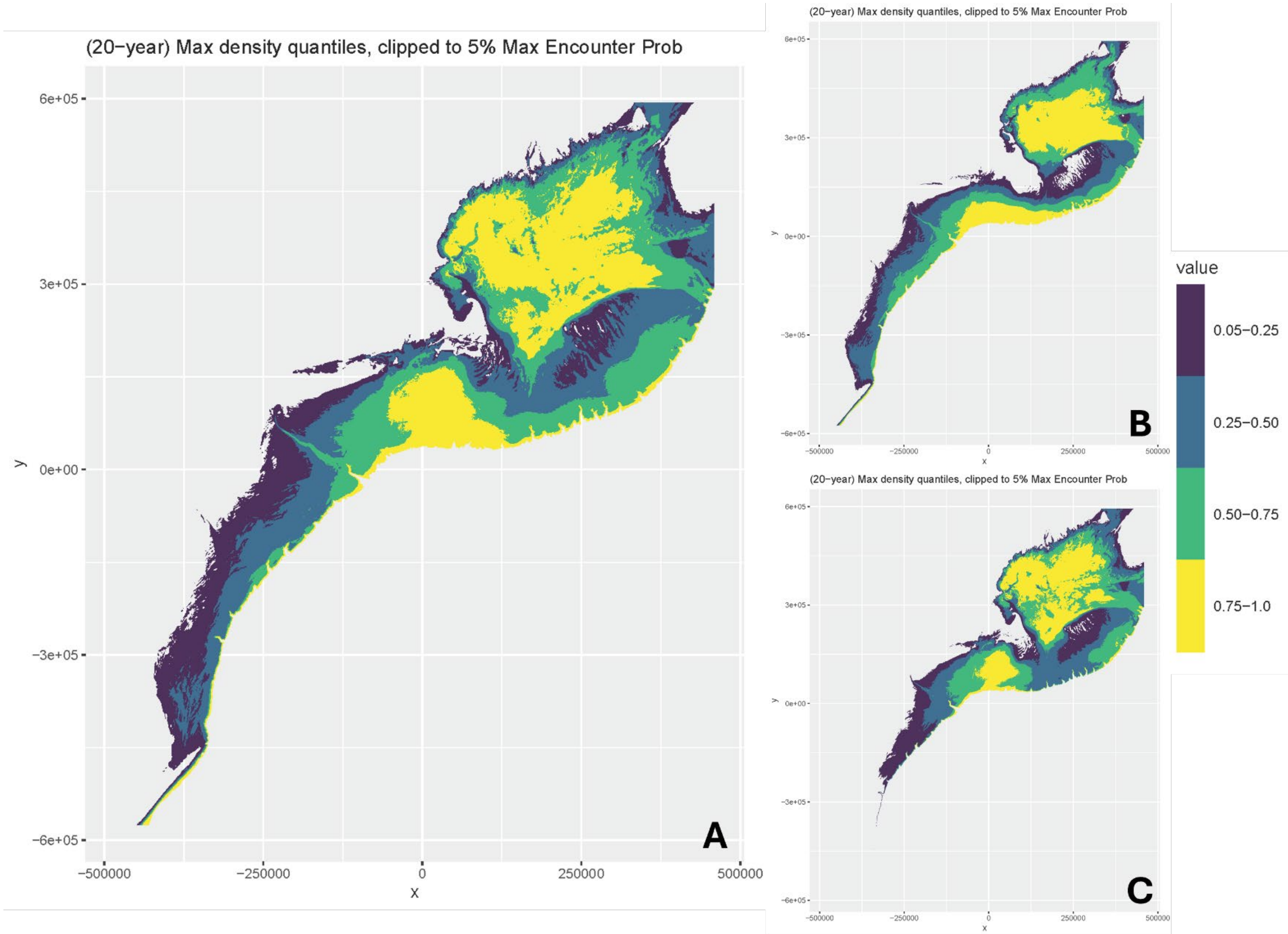

Figure 32. 22-year mean predicted density (species counts) for adult monkfish (*Lophius americanus*). Maps depict the maximum of the 22-year averages across (A) the full temporal range of the model (six months); and (C) fall survey months (September-November).

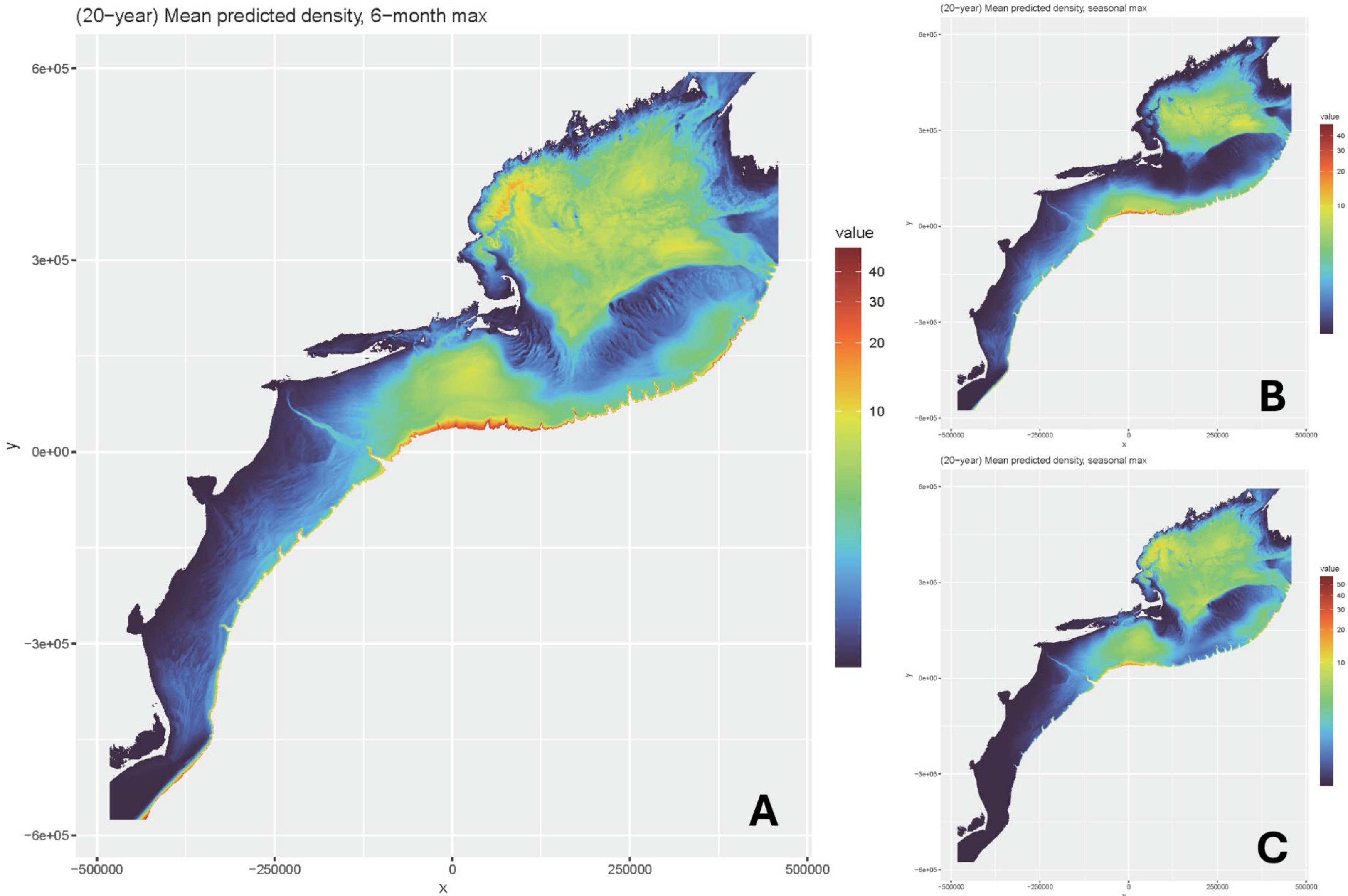

4.4 Barndoor skate

Figure 33. 22-year maximum predicted density (species counts) quantiles for pooled juvenile and adult barndoor skate (*Dipturus laevis*). Maps depict the maximum of the 22-year averages across (A) the full temporal range of the model (six months); and (C) fall survey months (September-November).

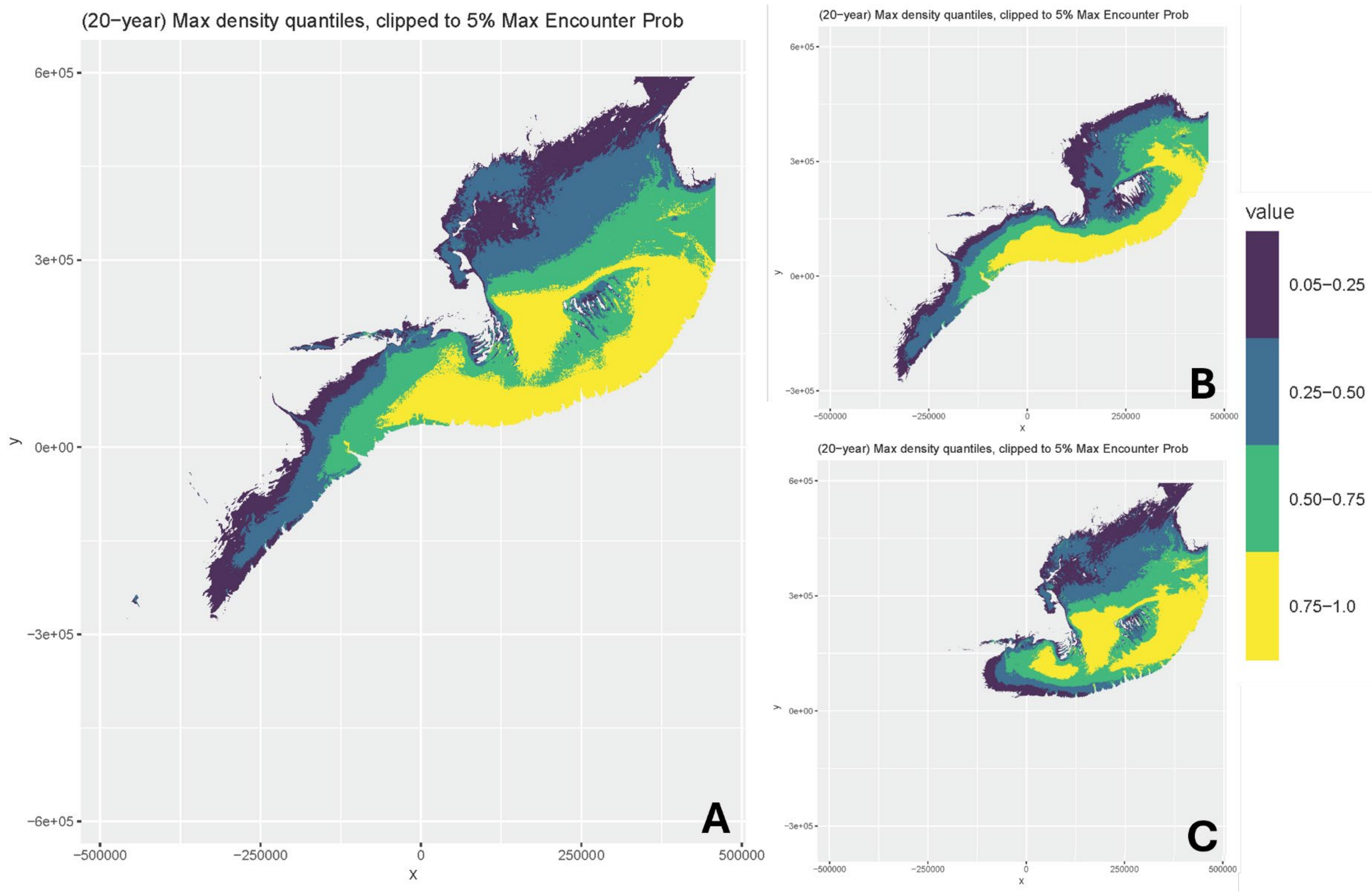

Figure 34. 22-year mean predicted density (species counts) for pooled juvenile and adult barndoor skate (*Dipturus laevis*). Maps depict the maximum of the 22-year averages across (A) the full temporal range of the model (six months); and (C) fall survey months (September-November).

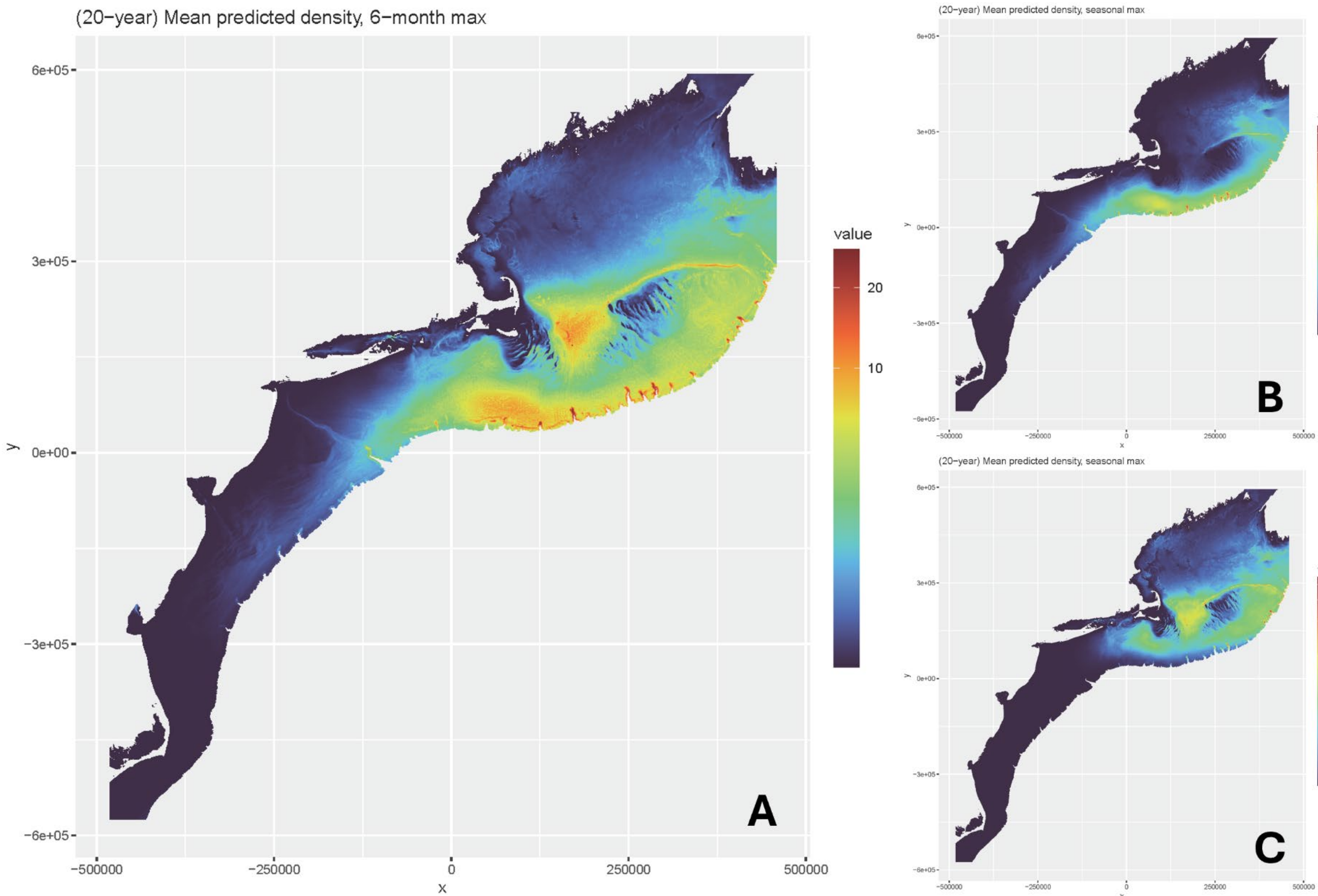

4.5 Clearnose skate

Figure 35. 22-year maximum predicted density (species counts) quantiles for juvenile clearnose skate (*Rostroraja eglanteria*). Maps depict the maximum of the 22-year averages across (A) the full temporal range of the model (six months); and (C) fall survey months (September-November).

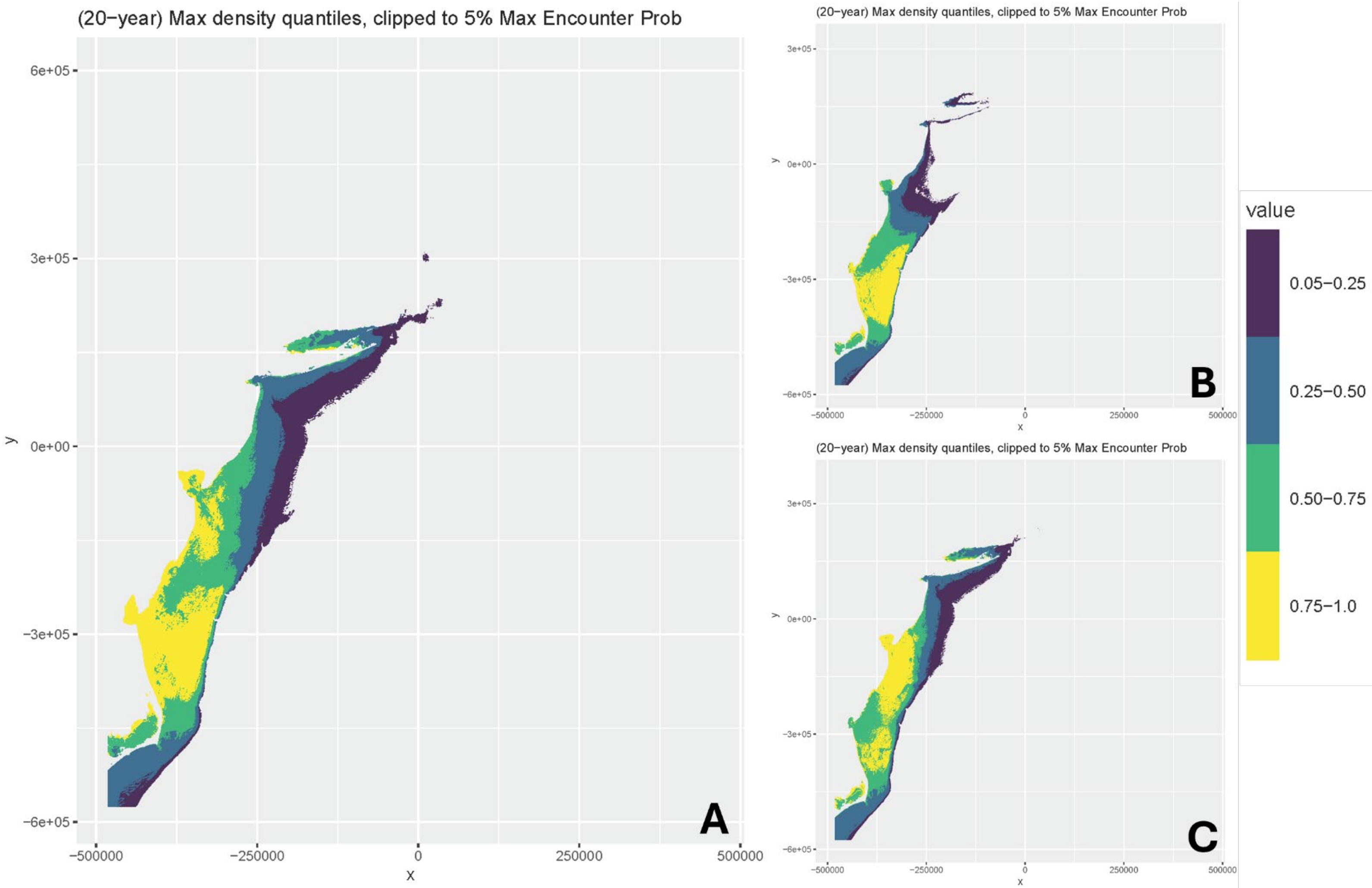

Figure 36. 22-year mean predicted density (species counts) for juvenile clearnose skate (*Rostroraja eglanteria*). Maps depict the maximum of the 22-year averages across (A) the full temporal range of the model (six months); and (C) fall survey months (September-November).

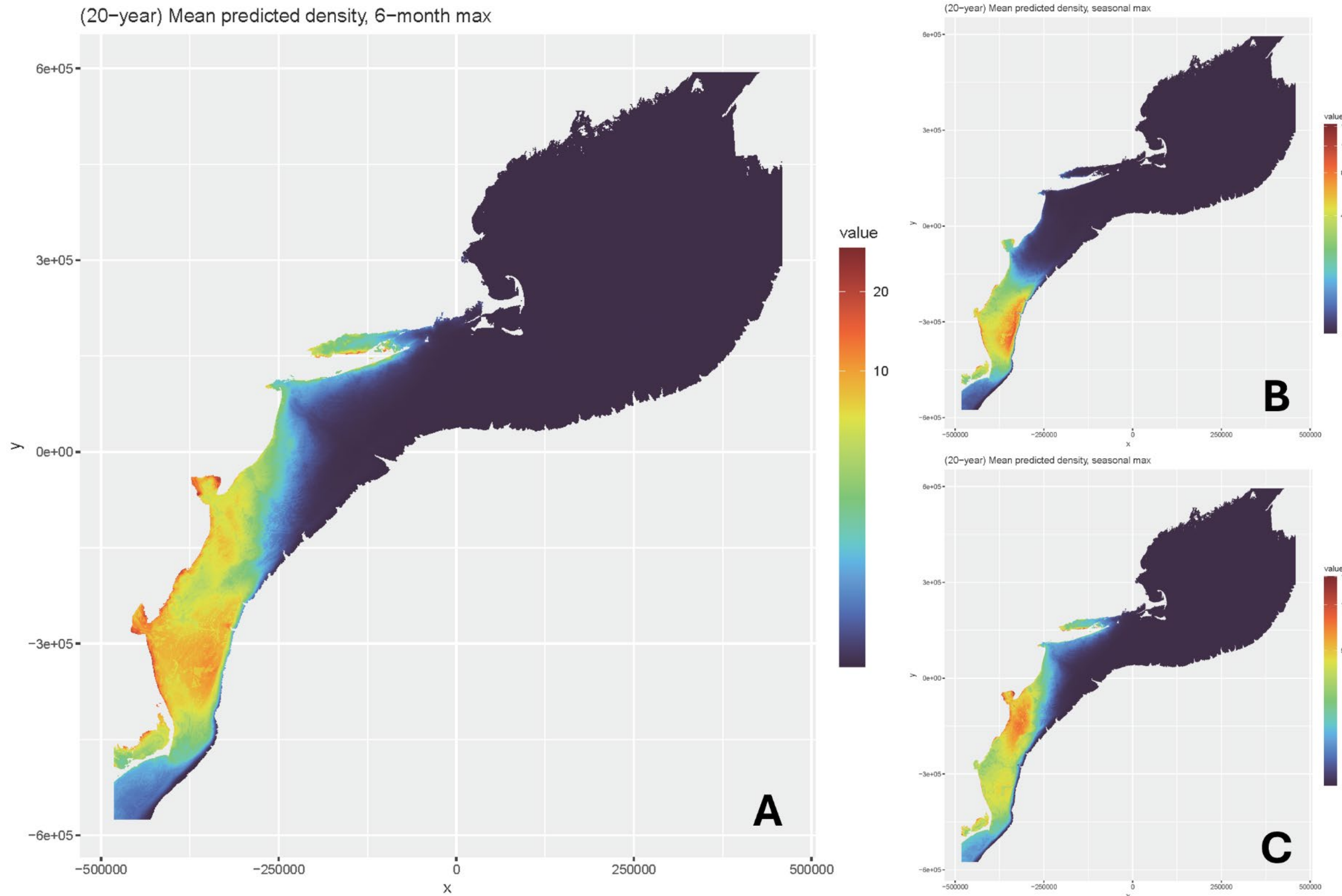

Figure 37. 22-year maximum predicted density (species counts) quantiles for adult clearnose skate (*Rostroraja eglanteria*). Maps depict the maximum of the 22-year averages across (A) the full temporal range of the model (six months); and (C) fall survey months (September-November).

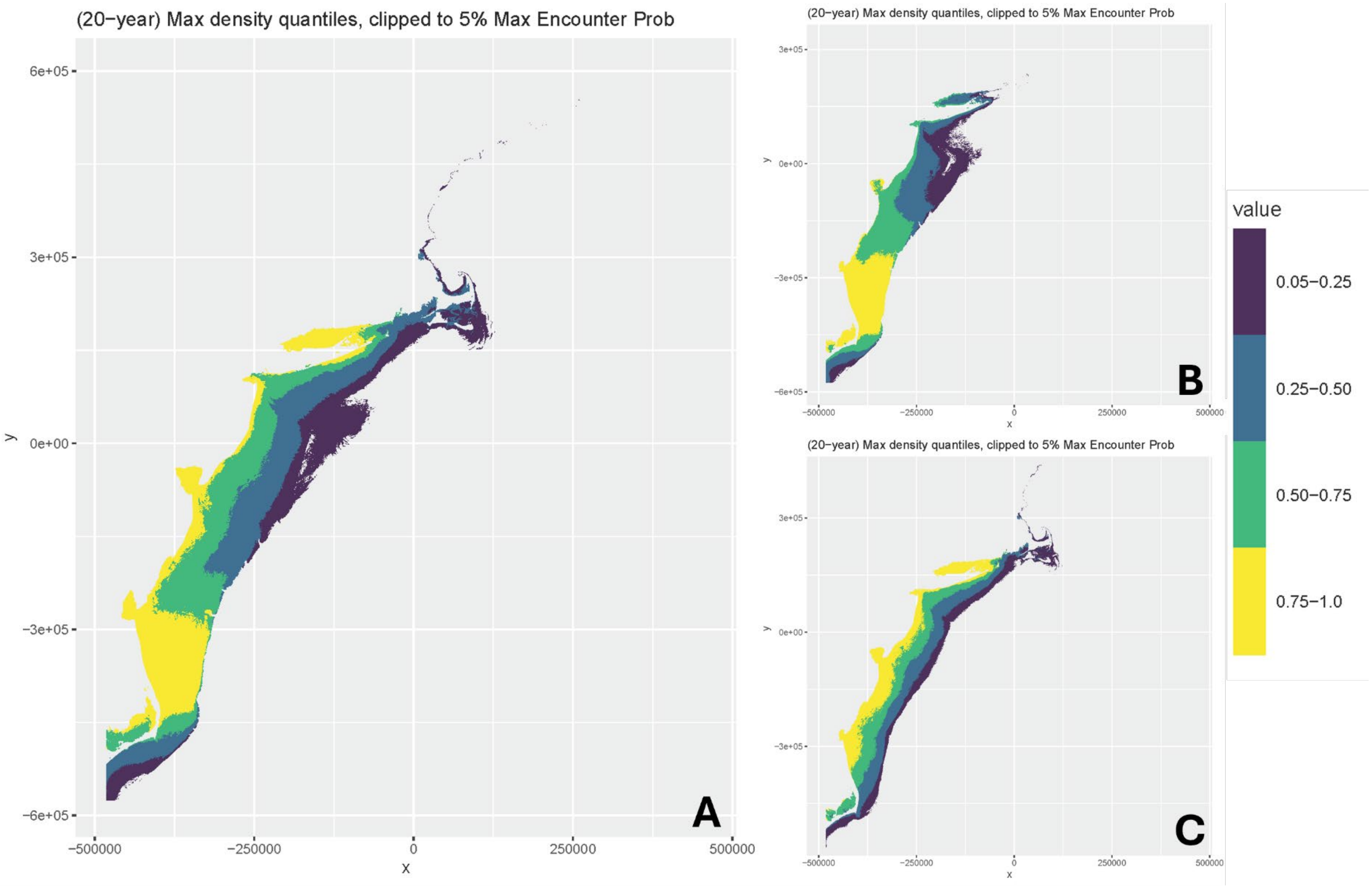

Figure 38. 22-year mean predicted density (species counts) for adult clearnose skate (*Rostroraja eglanteria*). Maps depict the maximum of the 22-year averages across (A) the full temporal range of the model (six months); and (C) fall survey months (September-November).

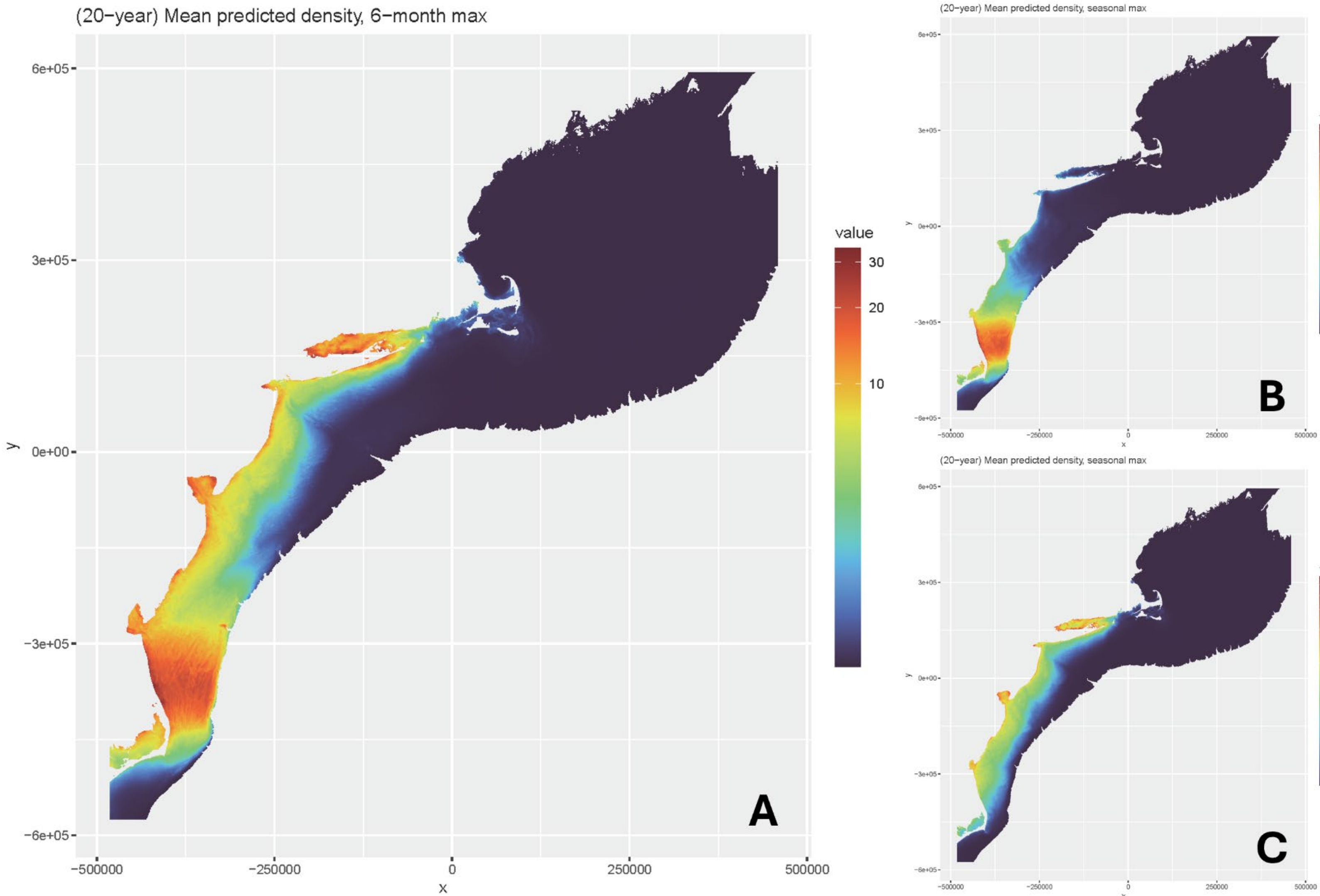

4.6 Little Skate

Figure 39. 22-year maximum predicted density (species counts) quantiles for juvenile little skate (*Leucoraja erinacea*). Maps depict the maximum of the 22-year averages across (A) the full temporal range of the model (six months); and (C) fall survey months (September-November).

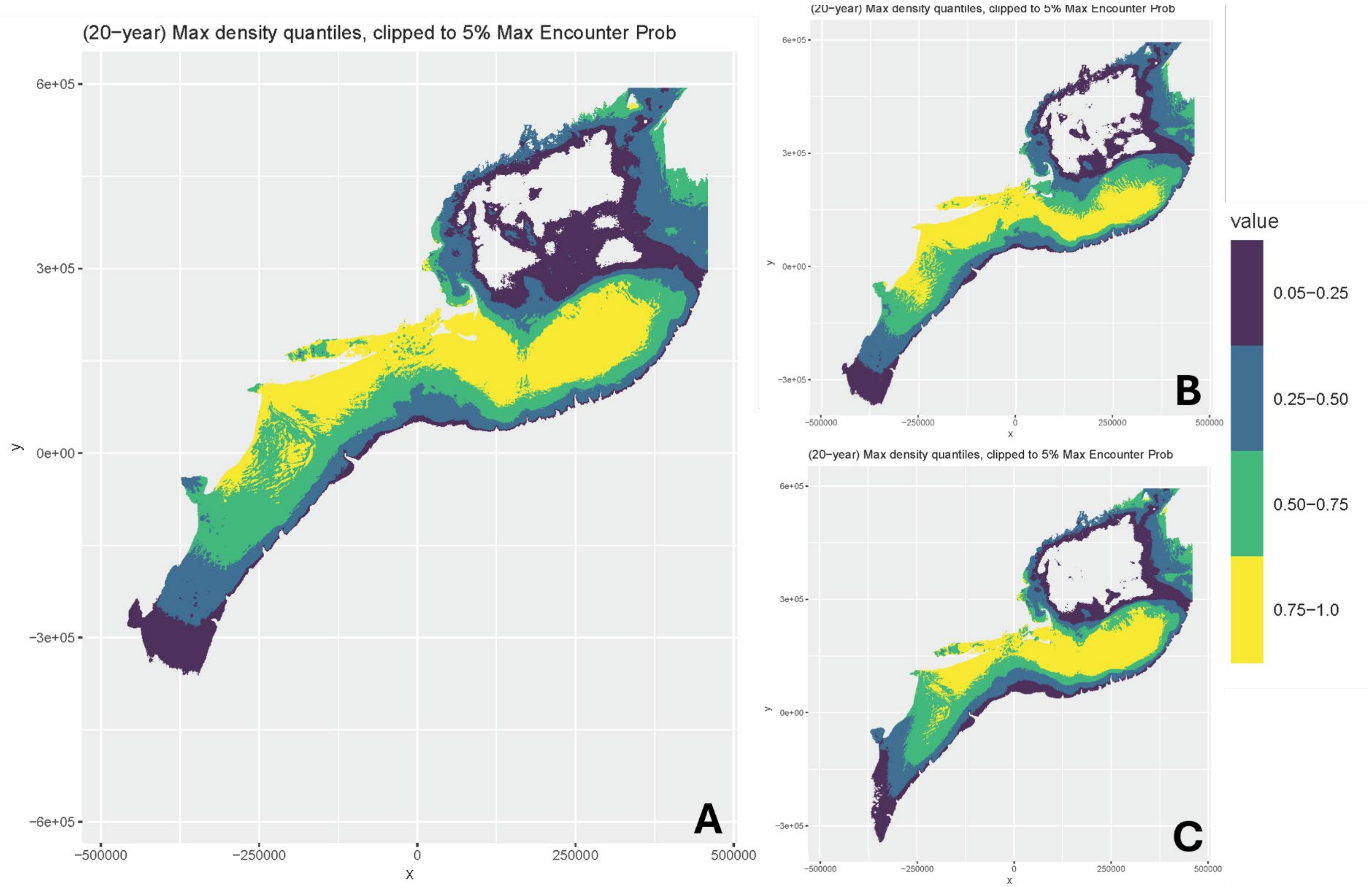

Figure 40. 22-year mean predicted density (species counts) for juvenile little skate (*Leucoraja erinacea*). Maps depict the maximum of the 22-year averages across (A) the full temporal range of the model (six months); and (C) fall survey months (September-November).

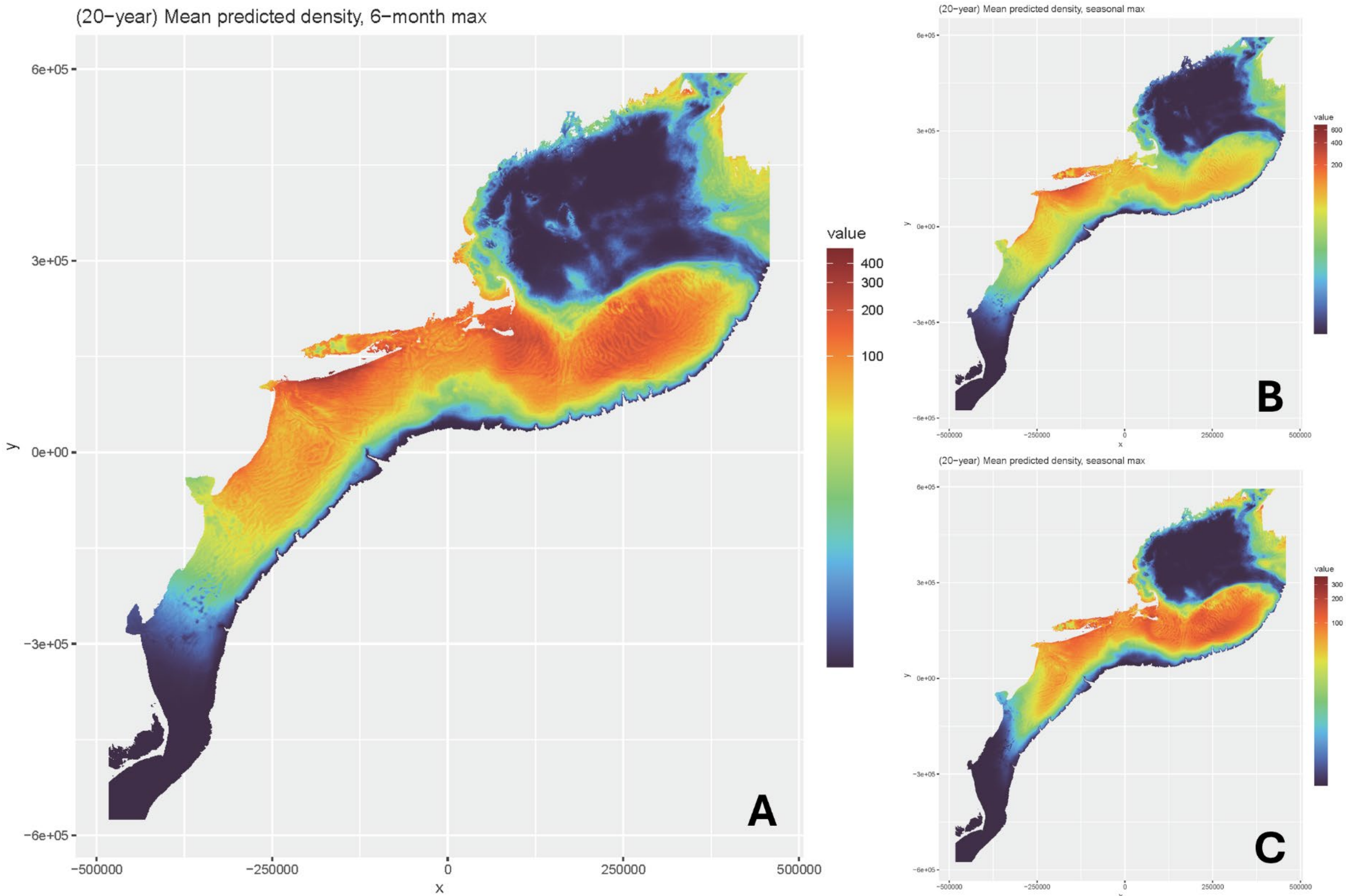

Figure 41. 22-year maximum predicted density (species counts) quantiles for adult little skate (*Leucoraja erinacea*). Maps depict the maximum of the 22-year averages across (A) the full temporal range of the model (six months); and (C) fall survey months (September-November).

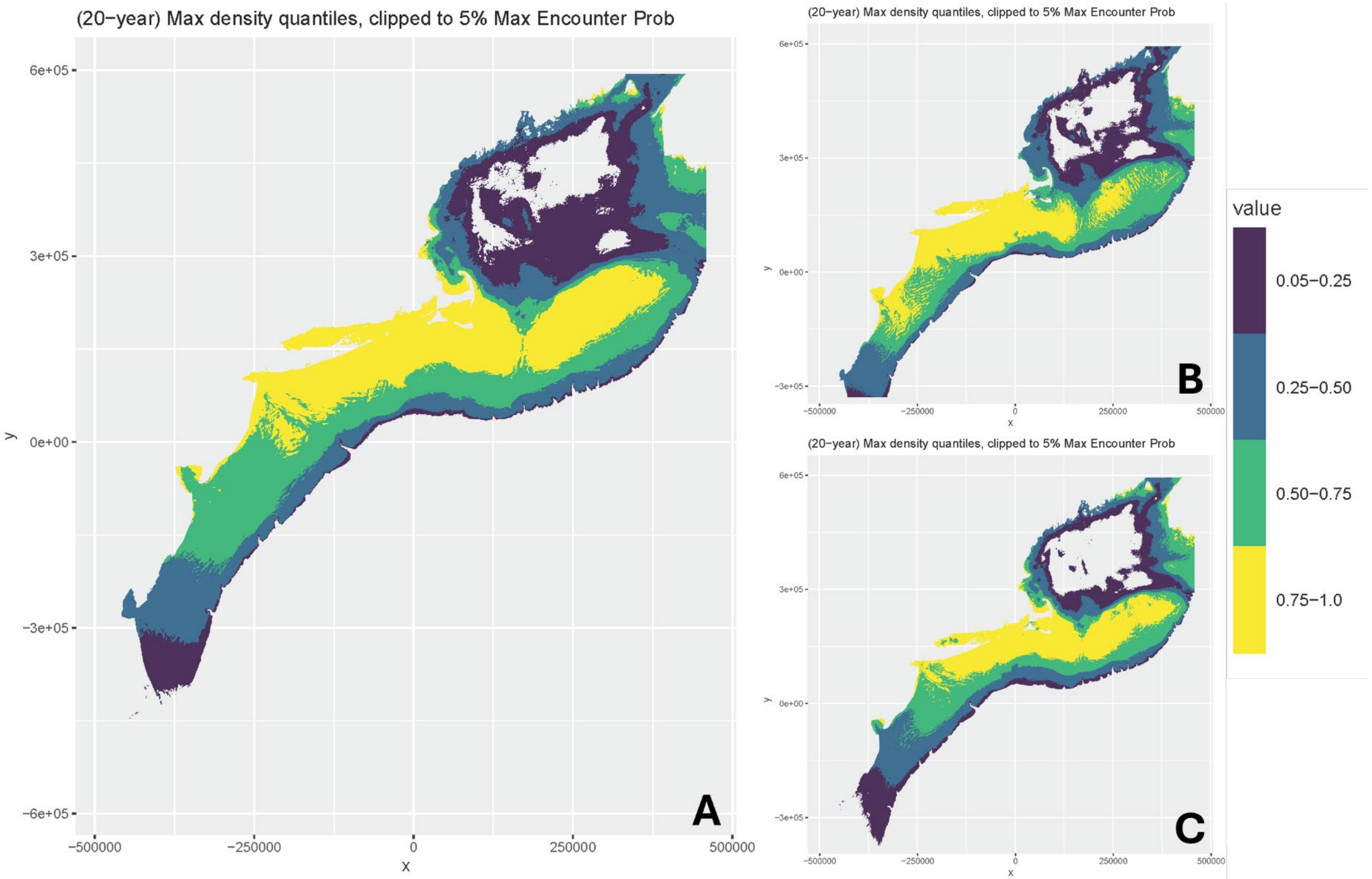

Figure 42. 22-year mean predicted density (species counts) for adult little skate (*Leucoraja erinacea*). Maps depict the maximum of the 22-year averages across (A) the full temporal range of the model (six months); and (C) fall survey months (September-November).

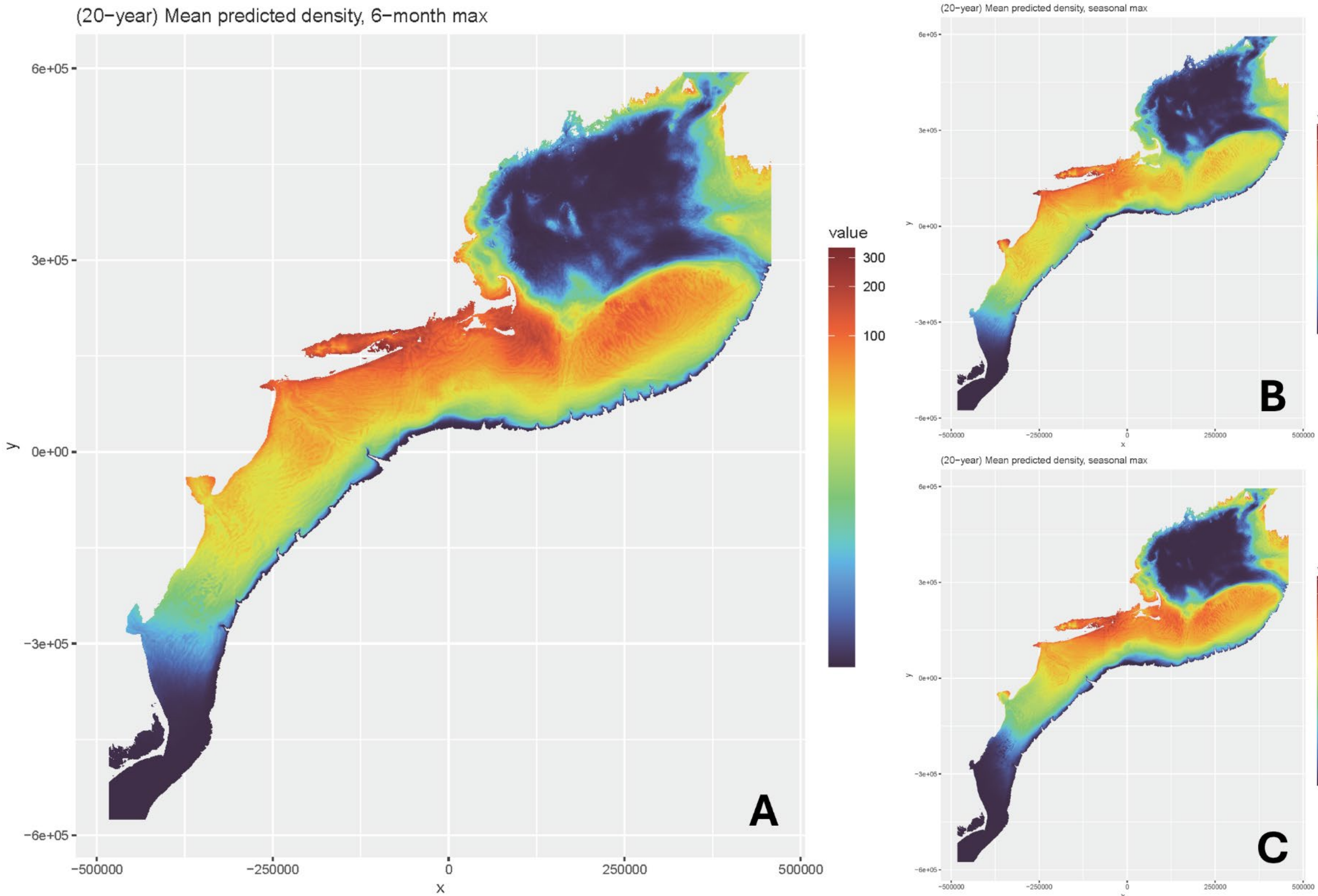

4.7 Rosette skate

Figure 43. 22-year maximum predicted density (species counts) quantiles for pooled juvenile and adult rosette skate (*Leucoraja garmani*). Maps depict the maximum of the 22-year averages across (A) the full temporal range of the model (six months); and (C) fall survey months (September-November).

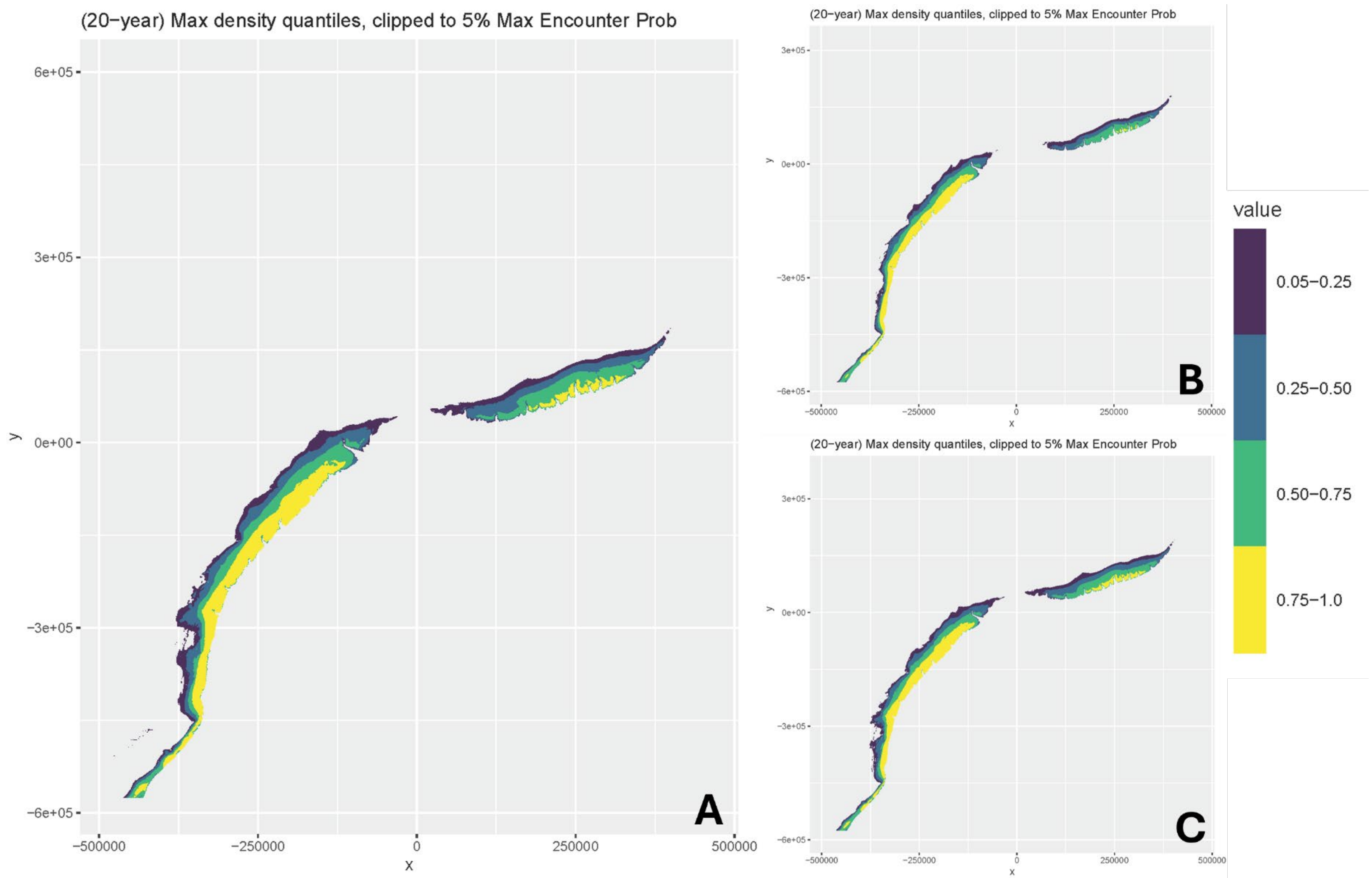

Figure 44. 22-year mean predicted density (species counts) for pooled juvenile and adult rosette skate (*Leucoraja garmani*). Maps depict the maximum of the 22-year averages across (A) the full temporal range of the model (six months); and (C) fall survey months (September-November).

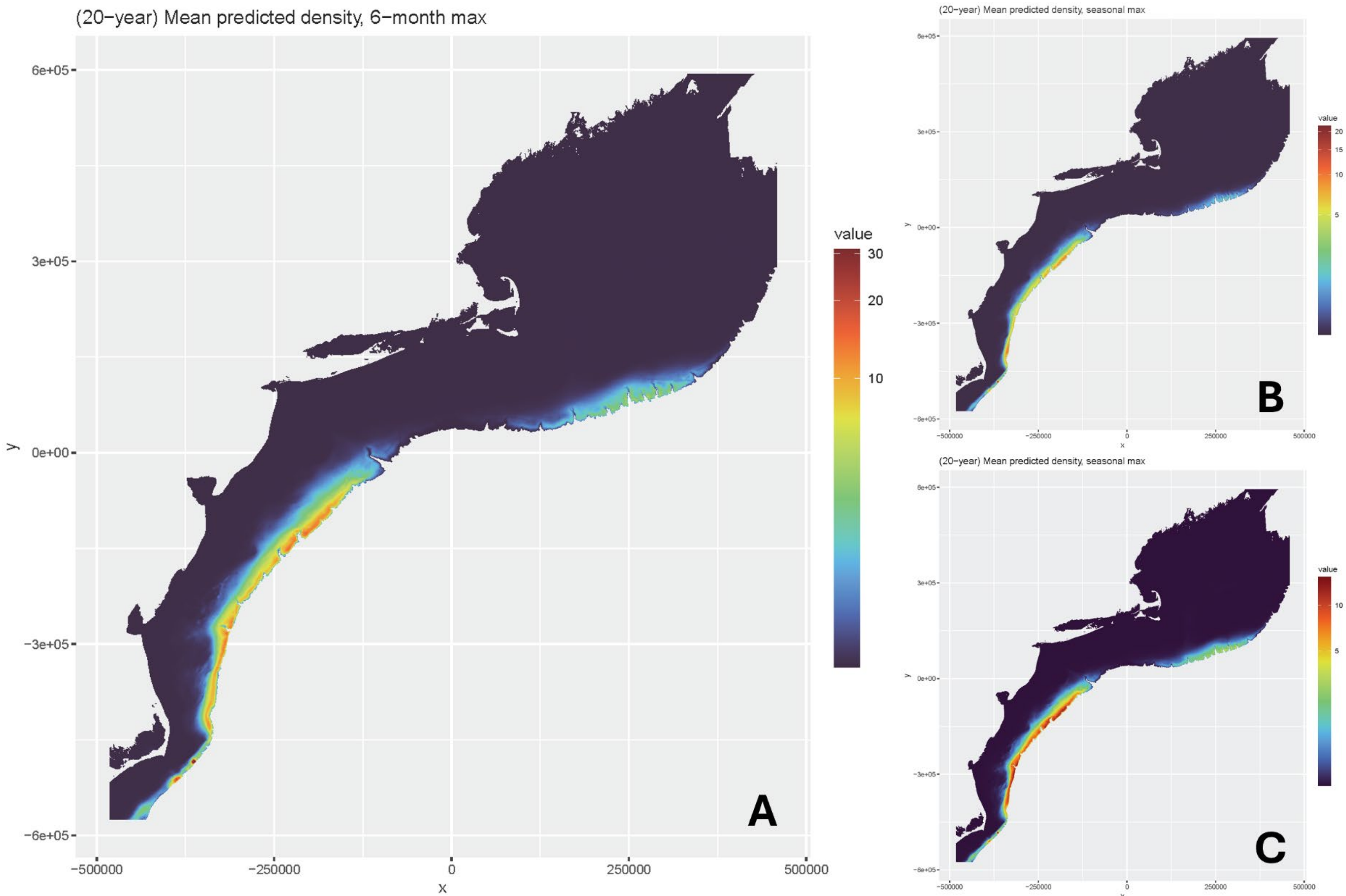

4.8 Smooth skate

Figure 45. 22-year maximum predicted density (species counts) quantiles for pooled juvenile and adult smooth skate (*Malacoraja senta*). Maps depict the maximum of the 22-year averages across (A) the full temporal range of the model (six months); and (C) fall survey months (September-November).

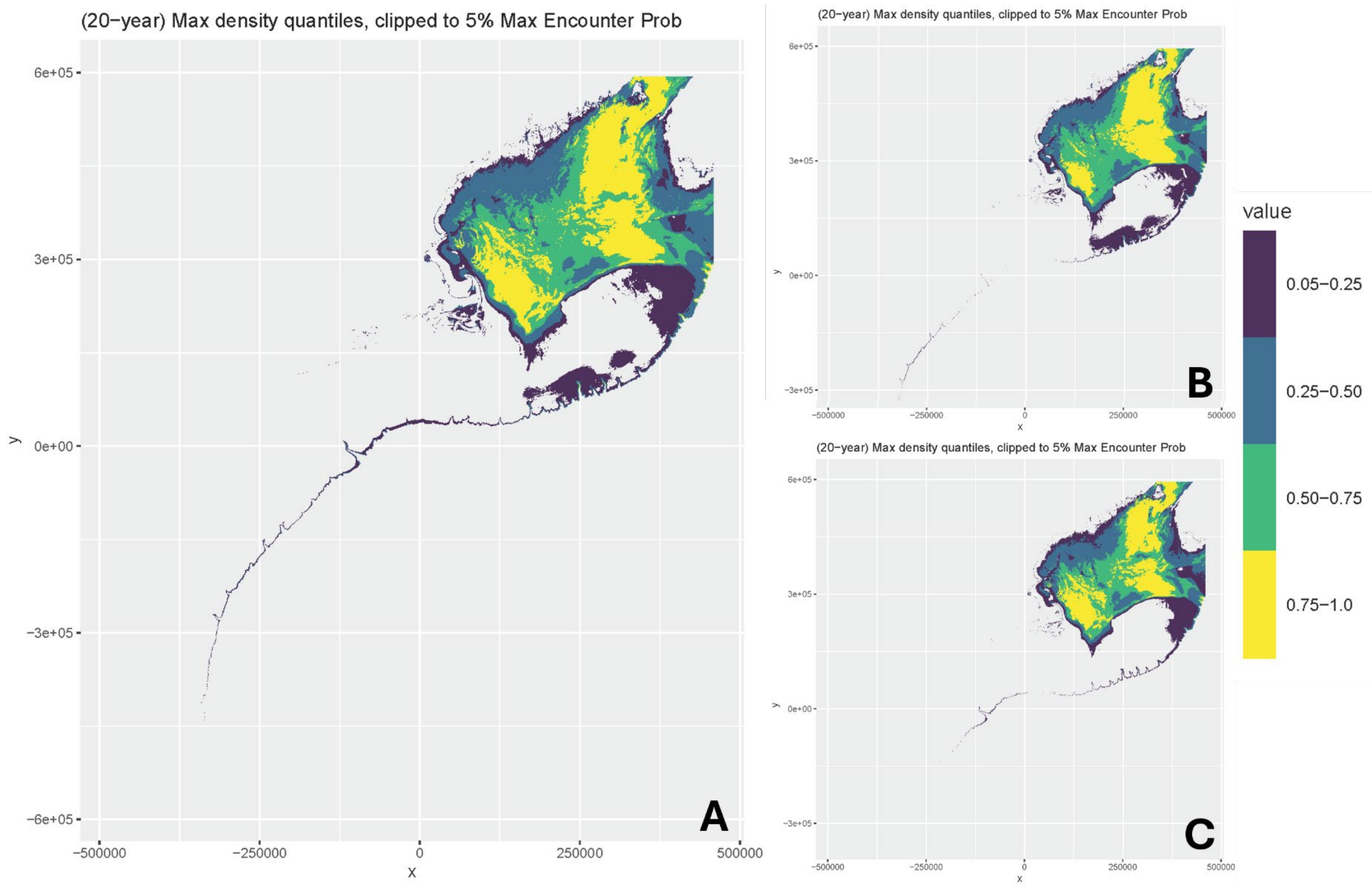

Figure 46. 22-year mean predicted density (species counts) for pooled juvenile and adult smooth skate (*Malacoraja senta*). Maps depict the maximum of the 22-year averages across (A) the full temporal range of the model (six months); and (C) fall survey months (September-November).

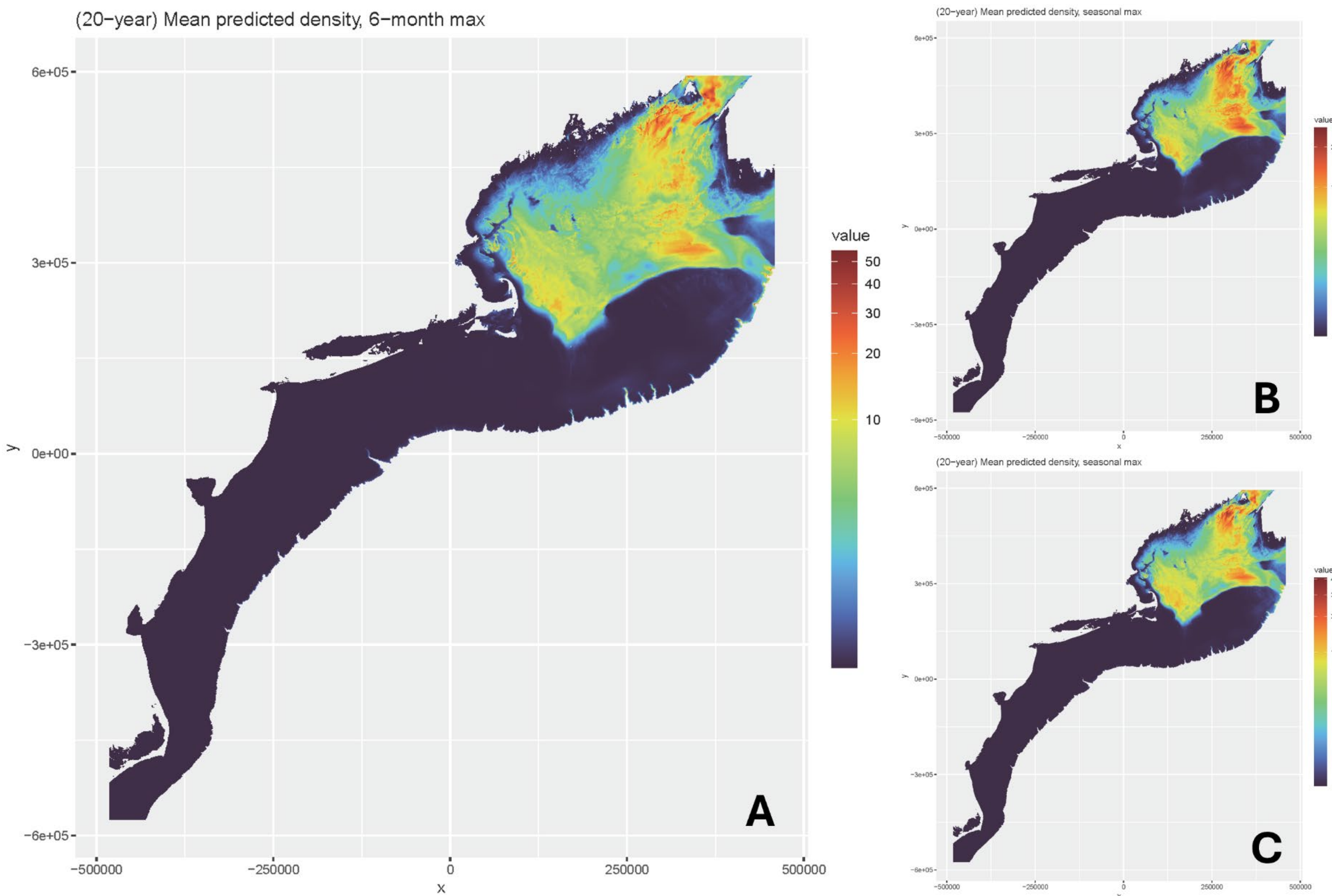

4.9 THORNY SKATE

Figure 47. 22-year maximum predicted density (species counts) quantiles for pooled juvenile and adult thorny skate (*Amblyraja radiata*). Maps depict the maximum of the 22-year averages across (A) the full temporal range of the model (six months); and (C) fall survey months (September-November).

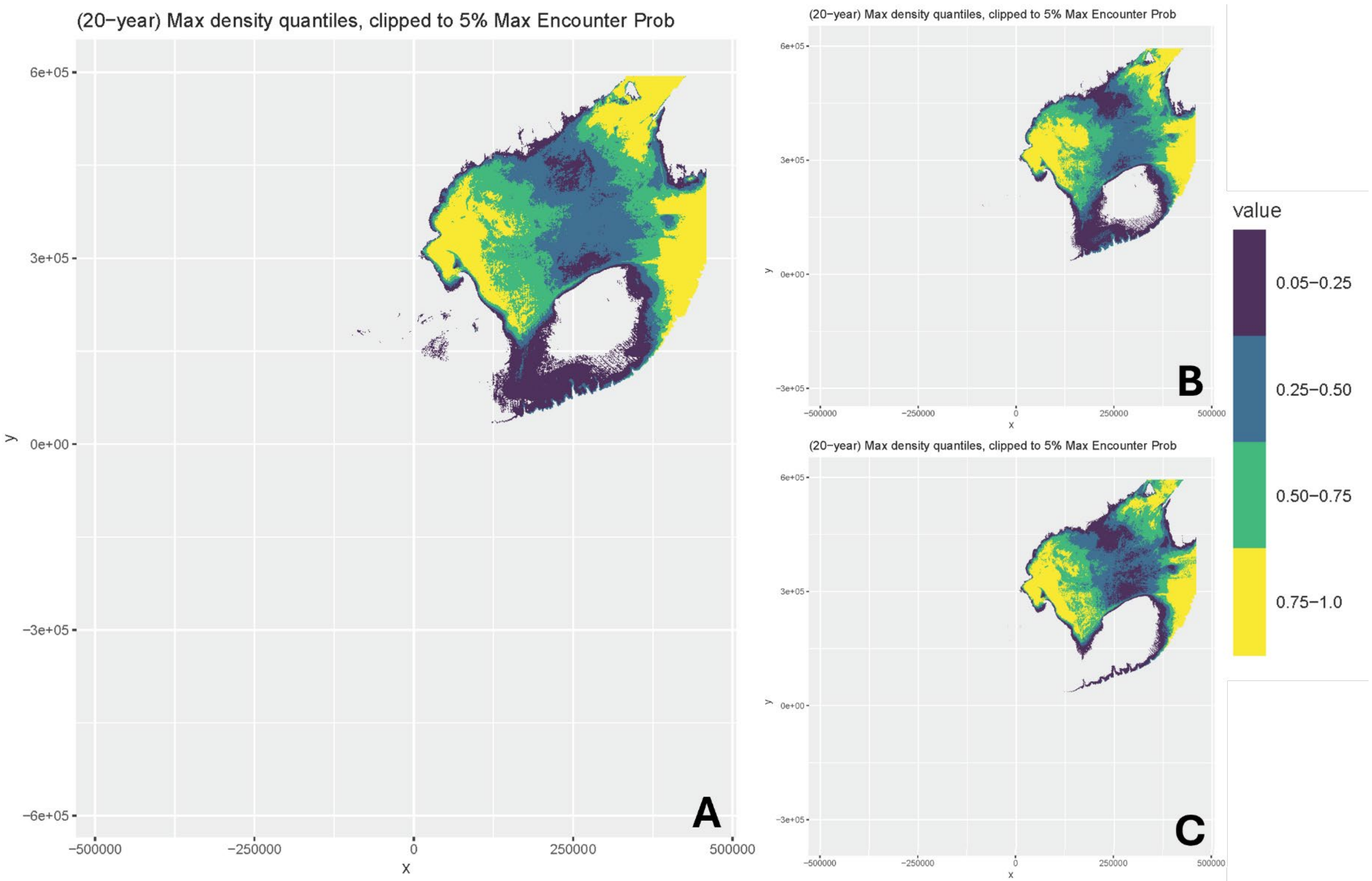

Figure 48. 22-year mean predicted density (species counts) for pooled juvenile and adult thorny skate (*Amblyraja radiata*). Maps depict the maximum of the 22-year averages across (A) the full temporal range of the model (six months); and (C) fall survey months (September-November).

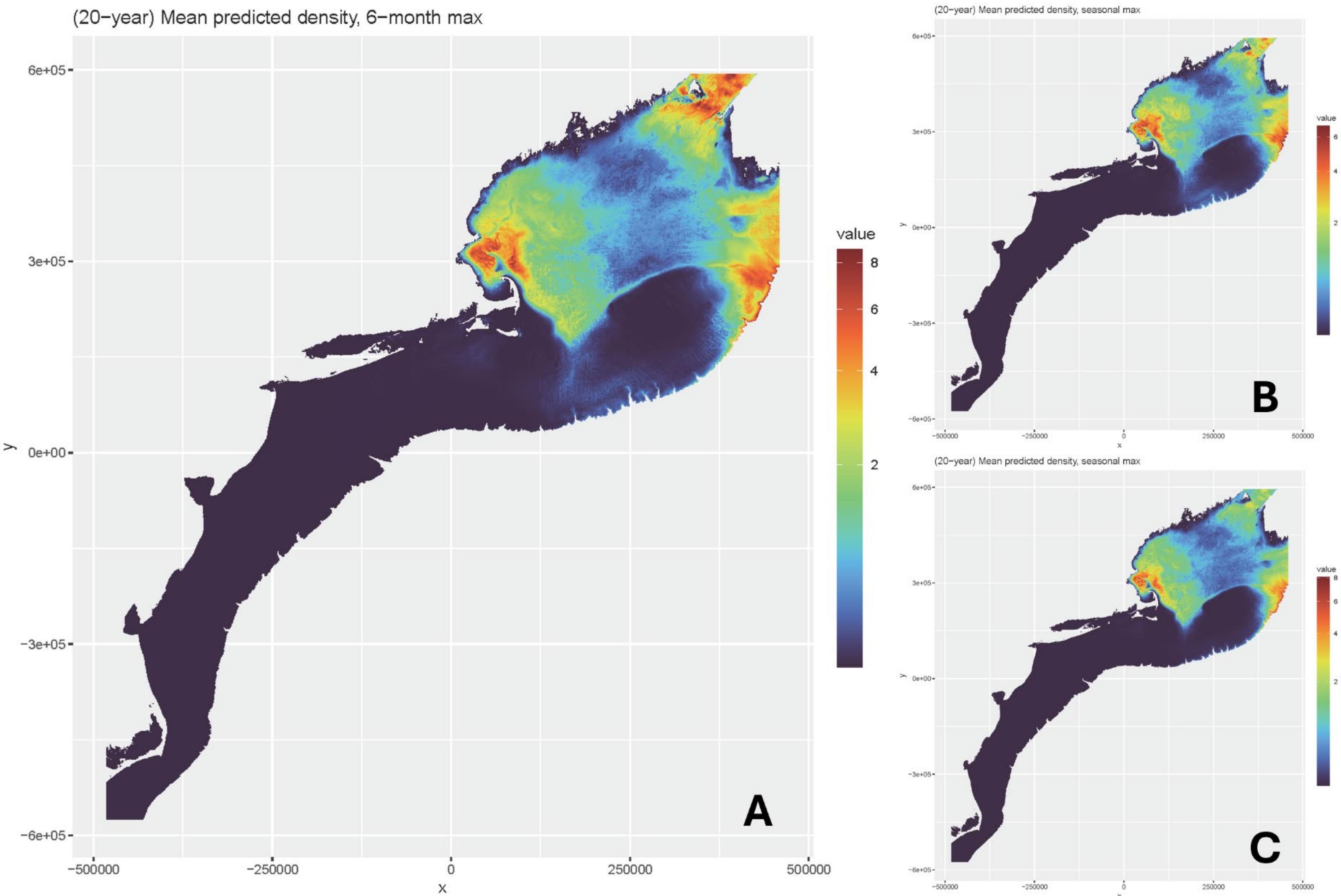

4.10 WINTER SKATE

Figure 49. 22-year maximum predicted density (species counts) quantiles for juvenile winter skate (*Leucoraja ocellata*). Maps depict the maximum of the 22-year averages across (A) the full temporal range of the model (six months); and (C) fall survey months (September-November).

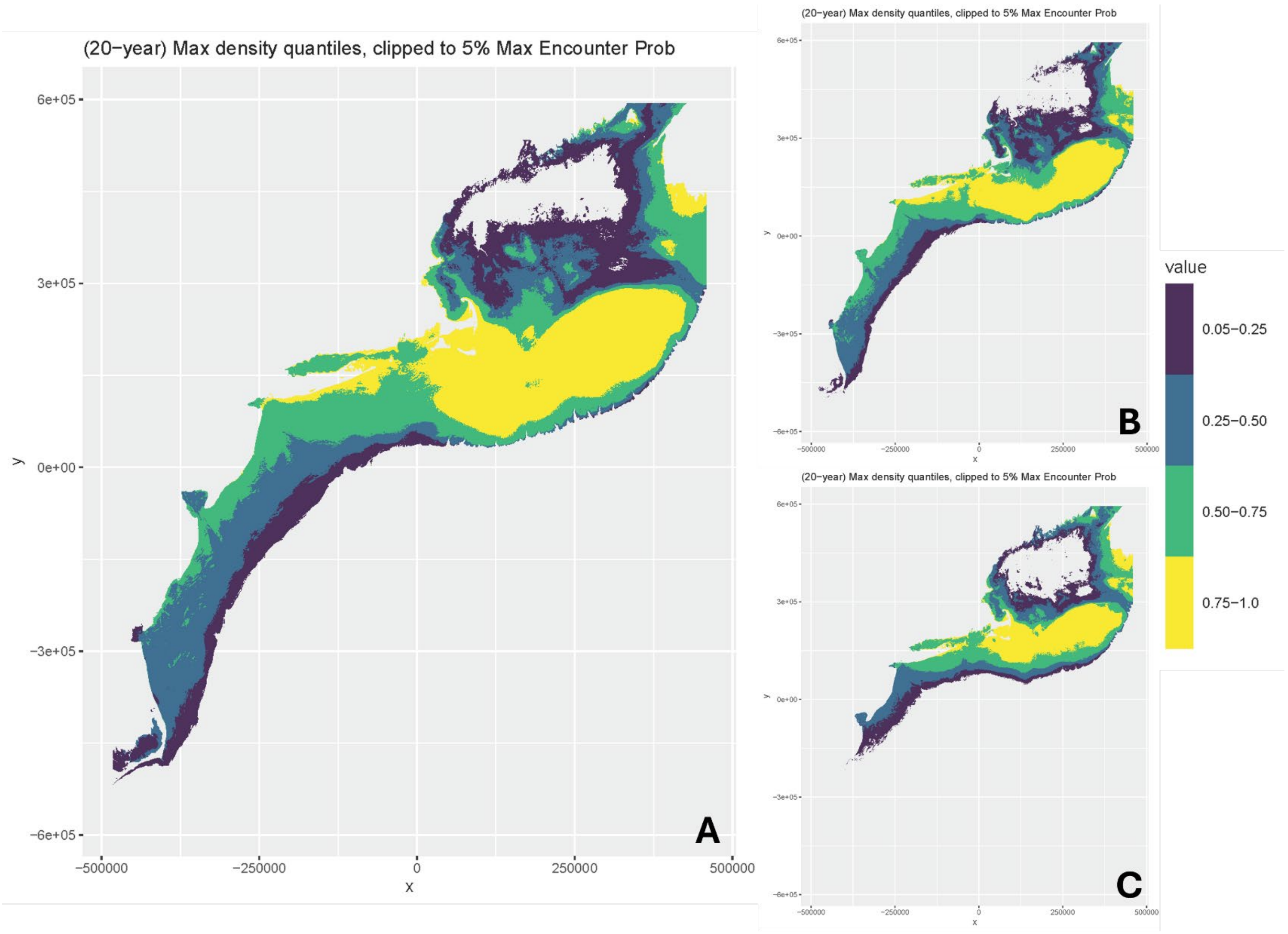

Figure 50. 22-year mean predicted density (species counts) for juvenile winter skate (*Leucoraja ocellata*). Maps depict the maximum of the 22-year averages across (A) the full temporal range of the model (six months); and (C) fall survey months (September-November).

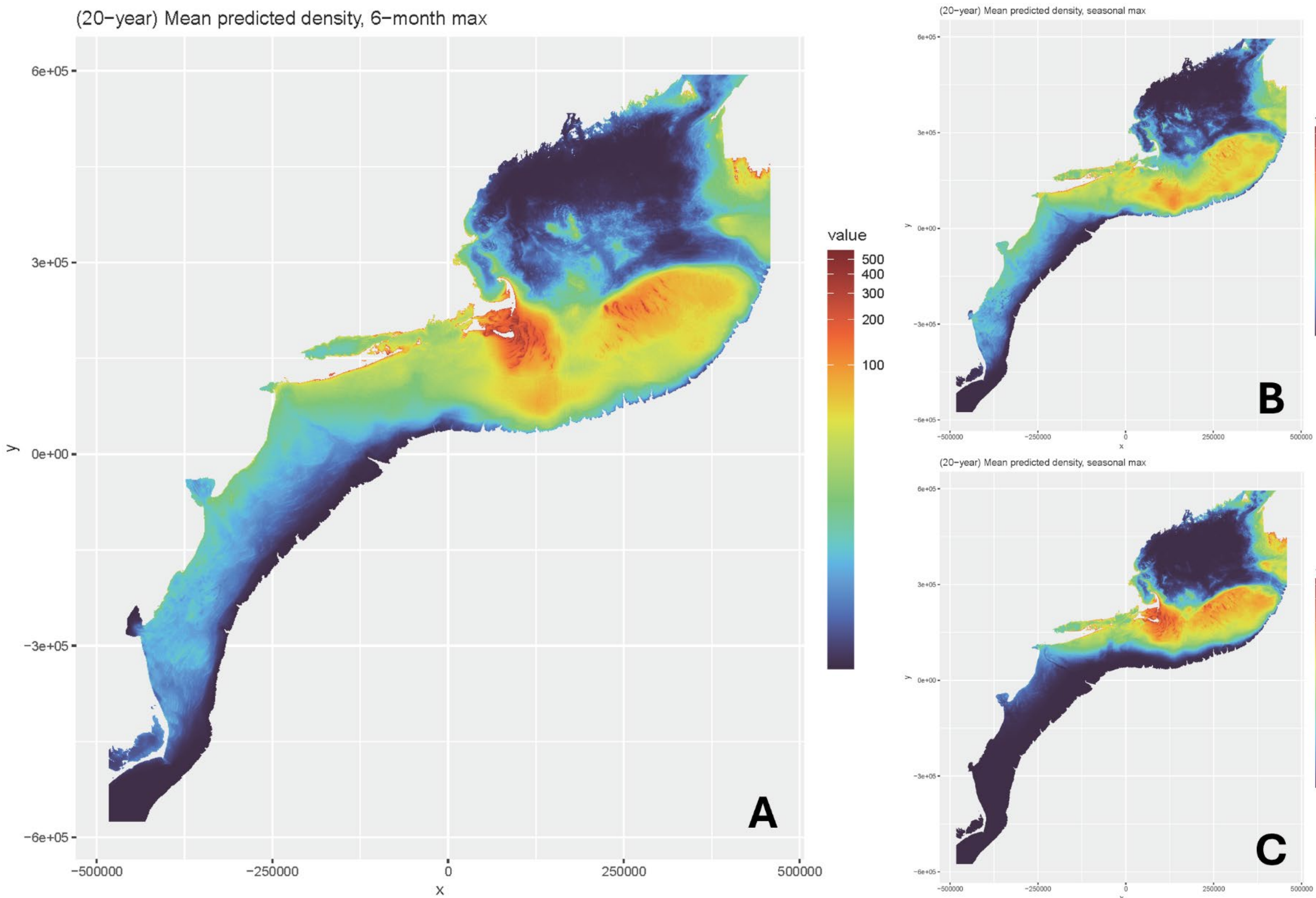

Figure 51. 22-year maximum predicted density (species counts) quantiles for adult winter skate (*Leucoraja ocellata*). Maps depict the maximum of the 22-year averages across (A) the full temporal range of the model (six months); and (C) fall survey months (September-November).

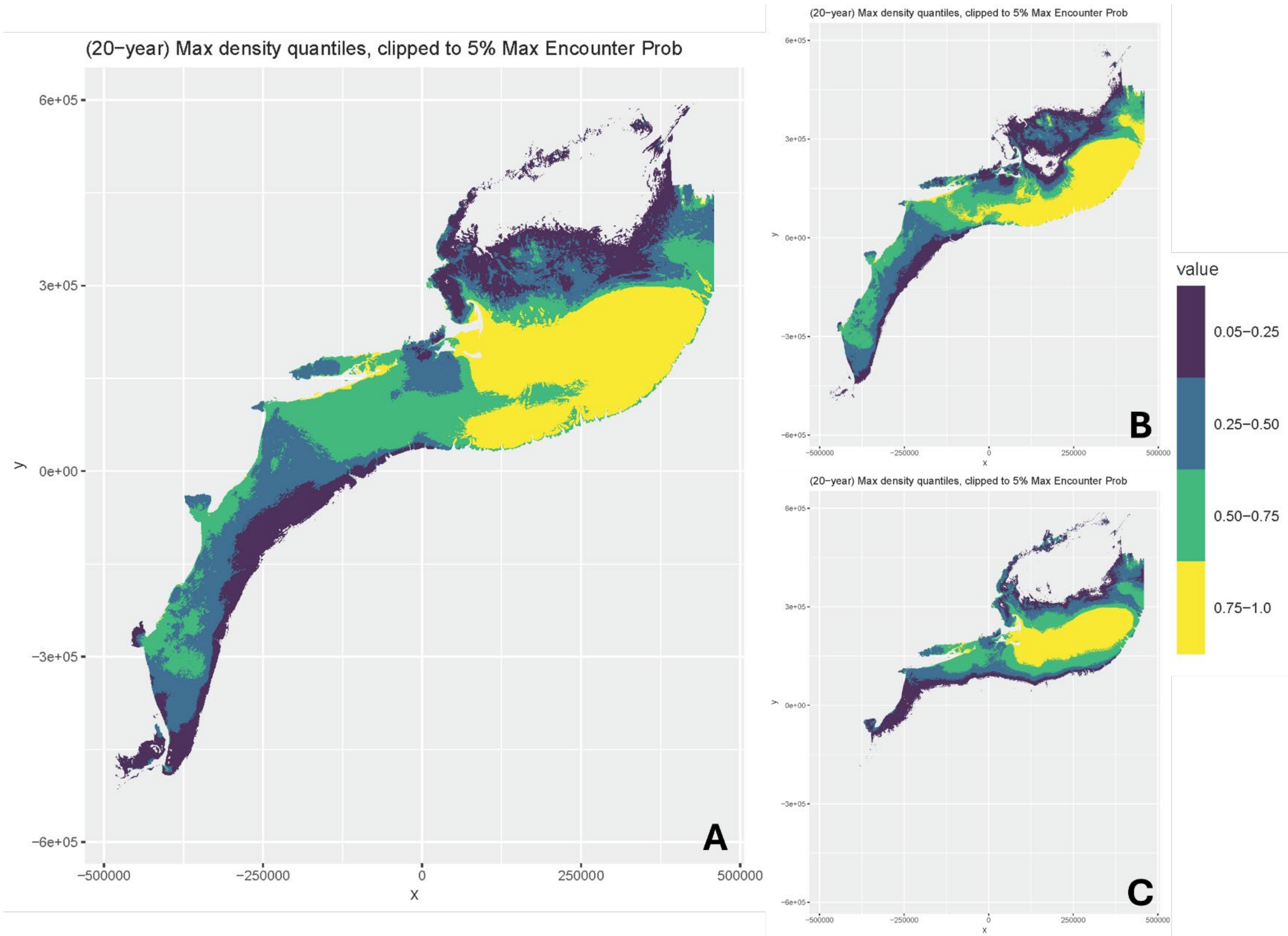

Figure 52. 22-year mean predicted density (species counts) for adult winter skate (*Leucoraja ocellata*). Maps depict the maximum of the 22-year averages across (A) the full temporal range of the model (six months); and (C) fall survey months (September-November).